New Phytologist

Mitochondrial alternative NADH dehydrogenases NDA1 and NDA2 promote survival of reoxygenation stress in Arabidopsis by safeguarding photosynthesis and limiting ROS generation

Jay Jethva[1], Sophie Lichtenauer[2], Romy Schmidt-Schippers[3], Anja Steffen-Heins[4], Gernot Poschet[5], Markus Wirtz[5], Joost T. van Dongen[6], Jürgen Eirich[2], Iris Finkemeier[2], Wolfgang Bilger[7], Markus Schwarzländer[2] and Margret Sauter[1†]

[1]Plant Developmental Biology and Plant Physiology, University of Kiel, 24118 Kiel, Germany; [2]Institute of Plant Biology and Biotechnology, University of Münster, 48143 Münster, Germany; [3]Plant Biotechnology, Bielefeld University, 33615 Bielefeld, Germany; [4]Institute of Human Nutrition and Food Science, University of Kiel, 24118 Kiel, Germany; [5]Centre for Organismal Studies, Heidelberg University, 69120 Heidelberg, Germany; [6]Institute of Biology I, RWTH Aachen University, 52074 Aachen, Germany; [7]Ecophysiology of Plants, University of Kiel, 24118 Kiel, Germany

Author for correspondence:
Jay Jethva
Email: jay.jethva@biology.ox.ac.uk

Received: *26 August 2022*
Accepted: *28 November 2022*

New Phytologist (2023) **238:** 96–112
doi: 10.1111/nph.18657

Key words: alternative electron transport chain, ANAC transcription factor, mitochondrial retrograde signaling, reactive oxygen species (ROS), reoxygenation after submergence.

Summary

- Plant submergence stress is a growing problem for global agriculture. During desubmergence, rising O_2 concentrations meet a highly reduced mitochondrial electron transport chain (mETC) in the cells. This combination favors the generation of reactive oxygen species (ROS) by the mitochondria, which at excess can cause damage. The cellular mechanisms underpinning the management of reoxygenation stress are not fully understood.
- We investigated the role of alternative NADH dehydrogenases (NDs), as components of the alternative mETC in Arabidopsis, in anoxia–reoxygenation stress management.
- Simultaneous loss of the matrix-facing NDs, NDA1 and NDA2, decreased seedling survival after reoxygenation, while overexpression increased survival. The absence of NDAs led to reduced maximum potential quantum efficiency of photosystem II linking the alternative mETC to photosynthetic function in the chloroplast. *NDA1* and *NDA2* were induced upon reoxygenation, and transcriptional activation of *NDA1* was controlled by the transcription factors ANAC016 and ANAC017 that bind to the mitochondrial dysfunction motif (MDM) in the *NDA1* promoter. The absence of NDA1 and NDA2 did not alter recovery of cytosolic ATP levels and NADH : NAD^+ ratio at reoxygenation. Rather, the absence of NDAs led to elevated ROS production, while their overexpression limited ROS.
- Our observations indicate that the control of ROS formation by the alternative mETC is important for photosynthetic recovery and for seedling survival of anoxia–reoxygenation stress.

Introduction

Submergence limits O_2 availability resulting in impaired respiration of plants (Sasidharan *et al.*, 2017). It can further limit photosynthesis by decreasing light exposure to green tissues. Both effects can jointly result in an energy crisis at the cellular level. When floodwaters retreat, a rise in oxygen and increased light intensity impose additional challenges on the plant (Yeung *et al.*, 2019). While adaptations to the submergence phase have been extensively studied, the reoxygenation phase has received less attention (Pucciariello & Perata, 2021). This study focuses on the acclimation that takes place in seedling shoots when transferred from anoxia in the dark to normoxia in the light.

Low oxygen leads to a reduced mitochondrial electron transport chain (mETC) flux, low adenylate energy charge, and high NADH : NAD^+ (Rasmusson *et al.*, 2008) which favors the formation of reactive oxygen species (ROS) at reoxygenation (Monk *et al.*, 1987; Biemelt *et al.*, 1998; Pavelic *et al.*, 2000; Garnczarska *et al.*, 2004; Yeung *et al.*, 2018; Jethva *et al.*, 2022). Excessive ROS production can cause oxidation of membrane lipids, proteins, nucleic acids, and carbohydrates (Blokhina *et al.*, 2000; Møller *et al.*, 2007, 2020; Santosa *et al.*, 2007). The fact that high rates of ROS production at reoxygenation pose a major threat to the plant is illustrated by the upregulation of antioxidant defense mechanisms in Arabidopsis, rice, soybean, and

†Deceased. Lead author.
In early January 2023 Margret Sauter passed away. Margret inspired with her creative ideas and open mind. She was a great mentor, a truly supportive colleague and a very good friend. Her work was not finished, but with her legacy she will continue to inspire scientists in the future.

Alternanthera philoxeroides (Luo *et al.*, 2010; Fukao *et al.*, 2011; Khan *et al.*, 2014; Khan & Komatsu, 2016; Yuan *et al.*, 2017; Yeung *et al.*, 2018).

Plant mitochondria show particularly high flexibility of possible electron paths and mechanisms to modulate the coupling between substrate oxidation and ATP synthesis. Apart from classical mETC, they possess an alternative respiratory chain (alternative mETC) composed of type II NAD(P)H dehydrogenases (NDs) and alternative oxidases (AOXs) (Vercesi *et al.*, 2006; Rasmusson *et al.*, 2008; Schertl & Braun, 2014; Wallström *et al.*, 2014; Vanlerberghe *et al.*, 2016; Selinski *et al.*, 2018; Møller *et al.*, 2021). The NDs bypass complex I and act as an alternative entry point for electrons to the mETC, while AOXs bypass complexes III and IV and act as alternative terminal oxidases to transfer electrons from ubiquinone (UQ) to molecular oxygen. The alternative mETC components do not pump any protons, which leads to a lower ATP yield per oxidized substrate.

NADH dehydrogenases are 50–60 kDa flavoproteins. *Arabidopsis thaliana* has seven NDs grouped into three clades: *NDA*, *NDB*, and *NDC* (Michalecka *et al.*, 2003). The NDA1, NDA2, and NDC are located at the inner surface of the inner mitochondrial membrane and oxidize matrix NADH (Moore *et al.*, 2003). Four NDB proteins (NDB1–4) face the outer surface of the inner mitochondrial membrane and oxidize NAD(P)H in the intermembrane space, which is in rapid exchange with the cytosolic NAD(P)H pools (Elhafez *et al.*, 2006; Sweetman *et al.*, 2019). Homologs of all three ND groups also exist in monocotyledonous plants (Rasmusson *et al.*, 2008).

The alternative mETC is presumed to act as an overflow mechanism that provides metabolic plasticity under environmental stress conditions. Alternative oxidase was reported to limit ROS production specifically when the mETC capacity is compromised (Vanlerberghe & McIntosh, 1997; Maxwell *et al.*, 1999; Camacho *et al.*, 2004; Cvetkovska & Vanlerberghe, 2013; Vishwakarma *et al.*, 2015; Popov *et al.*, 2021), but direct experimental evidence remains scarce (Rasmusson & Møller, 1991; Møller, 2001; Escobar *et al.*, 2004; Rasmusson *et al.*, 2008). While several studies have found AOX1a to be important in the tolerance to various stresses, the function of NDs remains less clear. A link between alternative mETC and photosynthesis is suggested by increased activity of alternative mETC components in photosynthetically active leaves (Michalecka *et al.*, 2003; Elhafez *et al.*, 2006) and impaired photosynthesis when either *AOX1a* or *NDB2* expression is compromised (Giraud *et al.*, 2008; Dahal & Vanlerberghe, 2017).

During reoxygenation in the light following anoxia in the dark, photosynthetic activity has to recover while the reduced redox centers of the mETC can pass electrons to molecular oxygen giving rise to elevated production rates of superoxide ($O_2^{\bullet-}$) that gives rise to other ROS in turn. Here, we analyzed the function and regulation of NDA1 and NDA2 in resilience of Arabidopsis leaves to an anoxia–reoxygenation stress. We show that mitochondria are a major subcellular source of ROS during reoxygenation and that the NDA-mediated alternative mETC safeguards photosynthetic function in the chloroplast by keeping cellular ROS in check.

Materials and Methods

Plant material, growth conditions, and plant treatments

Arabidopsis thaliana L. ecotype Columbia-0 (Col-0) was used for all analyses and as a genetic background for gain- and loss-of-function mutations. Arabidopsis seeds of mutant lines *nda1-1* (SALK_054530), *nda2-2* (GK-151F10), *anac016* (SALK_108782), and *anac017-1* (SALK_022174) were obtained from the Nottingham Arabidopsis Stock Centre (NASC, University of Nottingham, Loughborough, UK). All seeds were sterilized and germinated on either ½-strength Murashige & Skoog basal salt mix containing 0.1% or 1% sucrose (w/v) and 0.4% gelrite or 1% agar (w/v) or sown on a 1 : 1, sand : humus mixture covered with a nylon mesh. Seeds were stratified (4°C, 2 d) and then transferred to long-day conditions (16 h, 90 µmol m^{-2} s^{-1}, 8 h darkness). Anoxia and hypoxia treatments were carried out in the dark to avoid photosynthetic oxygen evolution in 7-l airtight acrylic boxes. For inhibitor treatments, seedlings were immersed in 5 mM 3-amino-triazole (AT) or 100 µM methyl viologen (MV) or 50 µM rotenone in water and shaken at 125 rpm for 3 h at 22°C in the light. More details are listed in Supporting Information Methods S1.

Cloning and transformation

DNA fragments were synthesized using Phusion™ High-Fidelity DNA Polymerase (Thermo Fisher Scientific, Waltham, MA, USA). Information about primers used to amplify DNA fragments is provided in Table S1. pENTR™/D-Topo® and pENTR1A™ (Thermo Fisher Scientific) were used as entry vectors, while the destination vectors pBGWFS7/pB7WG2,0 were used to generate overexpression, complementation, and reporter lines. Sequences were verified with Lightrun™ sequencing (GATC Biotech AG, Köln, Germany) of entry plasmids. Destination vectors with the desired DNA fragments were transformed into *Agrobacterium tumefaciens* strain EHA105, followed by plant transformation of Col-0 *via* floral dip (Clough & Bent, 1998).

Reverse transcription-quantitative real-time PCR

The Rotor-Gene SYBR® Green PCR Kit (Qiagen) and the Rotor-Gene® Q real-time PCR cycler (Qiagen) were used for quantitative expression analysis. The C_t values of the samples were normalized using Arabidopsis *ACTIN2* (*ACT2*, *At3g18780*) and *GLYCERALDEHYDE-3-PHOSPHATE DEHYDROGENASE C SUBUNIT* (*GAPC*, *At3g04120*) as reference genes with primers provided in Table S1. For each biological replicate, total RNA from shoots of 15–35 seedlings was pooled depending on genotype and treatment.

Mitochondria isolation and LC–MS/MS-based quantitative proteome analyses

Arabidopsis mitochondria were isolated from 2-wk-old seedlings as previously described (Escobar *et al.*, 2006). Proteins from

isolated mitochondria were reduced, alkylated, and digested. Further sample processing and LC–MS/MS data acquisition were performed as described previously (Lassowskat *et al.*, 2017). For more information, see Methods S2.

Survival assays

For the survival of anoxia/reoxygenation, 7-d-old plate-grown seedlings were treated as mentioned previously, and percentage of survival was calculated after 7 d of recovery. For submergence treatment, 4-wk-old soil-grown plants were fully submerged in a box (60 × 40 × 23 cm) filled with tap water equilibrated to 20°C for 3 d in the dark, subsequently desubmerged, and returned to long-day condition for 7 d before survival was scored.

Maximum quantum yield of PSII (F_V/F_M) and chlorophyll quantification

F_V/F_M was measured with an Imaging pulse-amplitude modulated (PAM) fluorometer IMAG-MAX/K (Walz, Effeltrich, Germany). Seedlings were dark adapted for 15 min before each measurement. Data were analyzed by Imaging Win v.2.41a (Walz). Total chlorophyll content was extracted and quantified as described in Lichtenthaler (1987).

ROS analysis using DAB and NBT staining and EPR spectroscopy

To detect H_2O_2 and superoxide, 3,3'-diaminobenzidin (DAB) and nitroblue tetrazolium (NBT) stainings were used according to methods described by Yang *et al.* (2014) with slight modifications. For more details, see Methods S3. For electron paramagnetic resonance (EPR) spectroscopy, shoots of 7-d-old seedlings were harvested and incubated in 2 mM of the spin probe *N*-(1-hydroxy-2,2,6,6-tetramethylpiperidin-4-yl)-2-methylpropanamide-hydrochloride (TMT-H) at 40°C for 90 min, and measurements were taken on a Bruker Elexsys E500 spectrometer (Bruker BioSpin GmbH, Rheinstetten, Germany). Further details are listed in Methods S3.

Measurement of ATP, NAD reduction level, and H_2O_2 concentration with fluorescent biosensors

For real-time analysis of ATP and NAD reduction levels in the cytosol of living seedlings, the fluorescent biosensors ATeam 1.03 nD/nA for $MgATP^{2-}$ (De Col *et al.*, 2017) and Peredox-mCherry for NADH : NAD^+ ratio (Hung *et al.*, 2011; Steinbeck *et al.*, 2020) were crossed into the respective backgrounds. Cytosolic and mitochondrial H_2O_2 dynamics were assessed using the genetically encoded biosensor roGFP2-Orp1, stably expressed in Col-0 wild-type (WT) background (Nietzel *et al.*, 2019). A multiwell plate reader-based fluorimetric assay was used similar to the approaches described previously (De Col *et al.*, 2017; Wagner *et al.*, 2019; Ugalde *et al.*, 2022) to analyze *in vivo* sensor responses during anoxia and reoxygenation. For more details, see Methods S4.

Transactivation and electrophoretic mobility shift assays

Preparation and transformation of Arabidopsis shoot protoplasts were performed according to Karimi *et al.* (2002). The truncated coding sequences of *ANAC013*, *ANAC016*, and *ANAC017* lacking the C-terminal transmembrane domain were cloned in the expression vector p2GW7.0. The *pNDA1:LUC* promoter:reporter construct was cloned in p2GWL7.0 (Karimi *et al.*, 2002). Five micrograms of each plasmid were co-transformed into Arabidopsis protoplasts. For normalization, a vector containing *35S:RLUC* was used for co-expression with ANACs. Dual-luciferase promoter assays (Promega) (Licausi *et al.*, 2011) were performed in four biological replicates, and luminescence was detected with a plate reader (Biotek Synergy MX; Agilent, Waldbronn, Germany).

For electromobility shift assays (EMSA), the truncated coding sequences of *ANAC013*, *ANAC016*, and *ANAC017* lacking the C-terminal transmembrane domain were fused to a FLAG tag by PCR and cloned into the pF3A WG Flexi vector (Promega). Subsequently, proteins were expressed in a TNT SP6 High-Yield Wheat Germ protein expression system (Promega) according to the manufacturer's protocol with 4 µg plasmid DNA. Successful expression of proteins was ensured by performing a Western blot against the FLAG-epitope tag. For gel-shift assays, IR-dye680-labeled probes were generated based on 33-bp-long regions derived from the *NDA1* promoter. DNA probes were generated by annealing forward and reverse oligonucleotides in equal molar ratios and slowly cooling them down from 95°C to 30°C (Table S2), diluting to a final concentration of 500 fmol and keeping them in amber tubes until use. Binding assays were performed using the Odyssey EMSA Buffer kit (Pierce, Rockford, IL, USA) for 2 h in the dark at 4°C. Subsequently, the reaction mixture was run on a 5% native polyacrylamide gel in TBE buffer, and bands were visualized with the ChemiDoc system (Bio-Rad). Details of GUS staining, adenylate measurement, and statistical analysis are listed in Methods S5–S7.

Results

NDA1 and NDA2 promote plant survival of reoxygenation

Publicly accessible transcriptome data indicated that *NDA1* and *NDA2* are specifically induced by reoxygenation in *A. thaliana* (Fig. S1). To functionally analyze the role of the NDA1 and NDA2 in response to anoxia and reoxygenation stress, we identified the loss-of-function lines *nda1-1* and *nda2-2* and generated the double knockout line *nda1-1 nda2-2* as well as lines with increased constitutive expression of *NDA1* and *NDA2* (Figs S2, S3). Survival of 16 h of anoxia followed by reoxygenation was scored in WT and mutant seedlings after 7 d of recovery (Figs 1a, S4). Wild-type, *nda1-1*, and *nda2-2* seedlings had a mortality rate of *c.* 55%. Mortality increased to *c.* 90% in *nda1-1 nda2-2* seedlings, whereas increased constitutive expression of *NDA1* or *NDA2* reduced mortality to 10–20%. The dramatic phenotype indicates that maintenance of the NDA-driven alternative mETC is crucial for seedling survival of anoxia and/or postanoxic stress

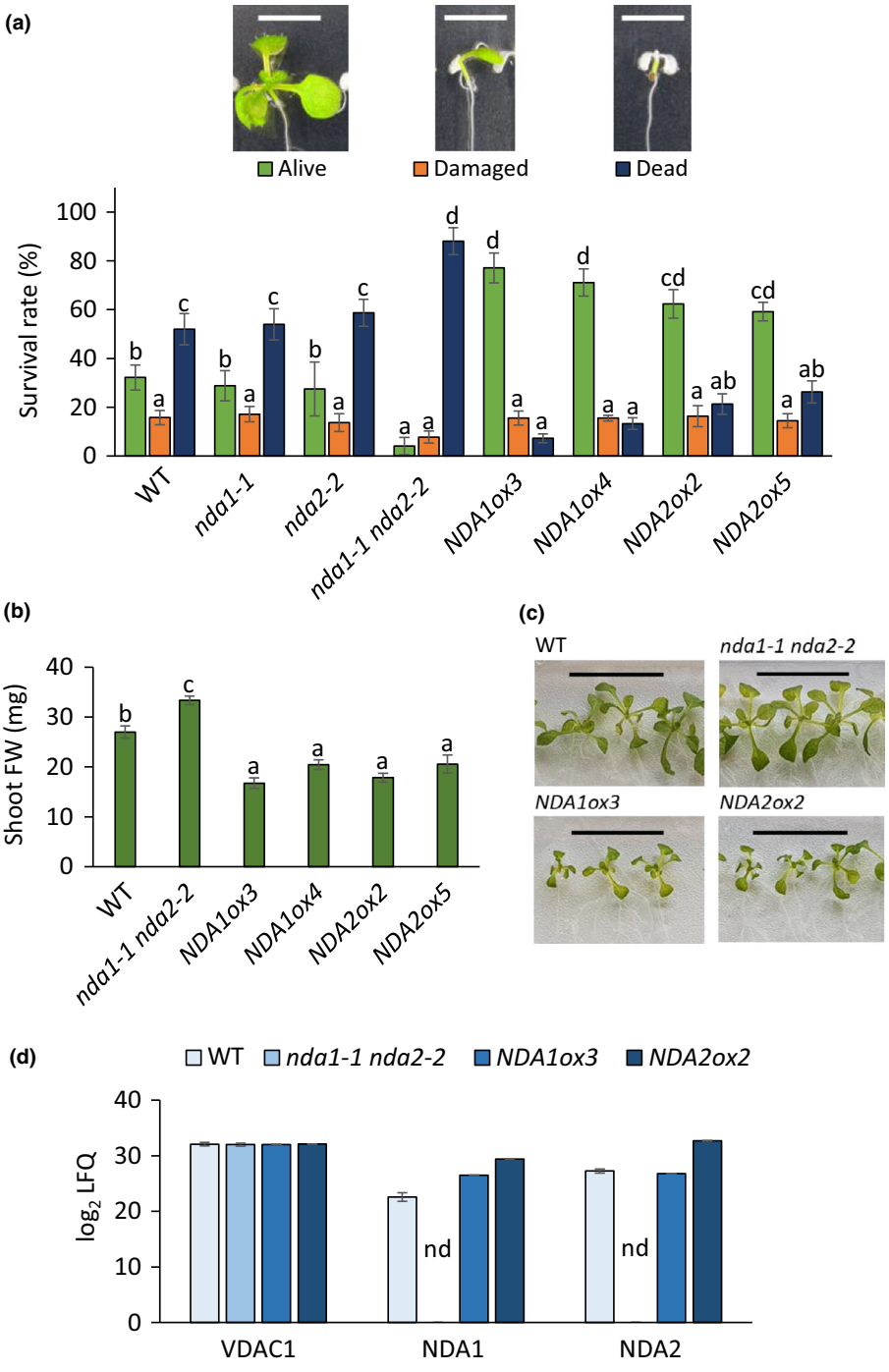

Fig. 1 *NDA1* and *NDA2* are required for seedling survival of reoxygenation. (a) Seven-day-old wild-type (WT) and *NDA* mutant seedlings were exposed to 16-h anoxia in the dark and then returned to long-day conditions for 7 d of recovery. The percentage of alive, damaged, and dead seedlings was determined. Results are means (±SE, $n = 9$–15, one-way ANOVA with Tukey's test, $P < 0.05$) obtained in three independent experiments. Representative pictures of plant phenotypes at the end of the recovery phase are shown on top of the graph. Bar, 5 mm. (b) Average shoot fresh weight of 14-d-old seedlings grown in long-day conditions (±SE, $n = 35$–42, one-way ANOVA with Tukey's test, $P < 0.05$) analyzed in three independent experiments. Different letters indicate statistically different groups. (c) Representative pictures of 14-d-old WT, *nda1-1 nda2-2*, *NDA1ox3*, and *NDA2ox2* seedlings. Bar, 2 cm. (d) The calculated $\log_2$ LFQ (label-free quantitation) intensities of Voltage-Dependent Anion Channel (VDAC1), NDA1, and NDA2 protein were determined in mitochondria isolated from WT, *nda1-1 nda2-2*, *NDA1ox3* and *NDA2ox2* shoots (±SE, $n = 3$ for WT and *nda1-1 nda2-2* and $n = 1$ for *NDA1ox3* and *NDA2ox2*). No statistical analysis was performed because peptides of proteins were not detected (nd) in *nda1-1 nda2-2* and the mitochondrial proteome of just one replicate was assessed for each of the *NDA1ox* lines.

with *NDA1* and *NDA2* acting redundantly. It needs to be added that the experimental conditions used here will drastically deplete atmospheric oxygen. Yet, the removal of oxygen from the plant tissue is unlikely to be quantitative. Hence, the conditions that we refer to as anoxia throughout this work plausibly represent severe hypoxia rather than the total absence of oxygen at the tissue and cell level. Residual oxygen amounts within cells, and tissues are likely to be very low but are hard to reliably quantify. While this is a limitation that needs to be considered, the standardized nature of the treatment provides a tangible model for severe low-oxygen stress.

NDA genes are expressed not only during reoxygenation but also under normoxic conditions (Fig. 2). Since NDAs provide a bypass to the proton pumping by complex I, their activity decreases the ratio of ATP molecules synthesized per NADH oxidized decreasing energy conservation efficiency. Indeed, under nonstressed conditions, NDA-mediated alternative electron transport was maintained at a metabolic cost that was reflected in reduced shoot biomass in *NDA1ox3* and *NDA2ox2* and elevated shoot biomass in *nda1-1 nda2-2* seedlings compared with WT (Fig. 1b,c).

To verify a functional link between *NDA* genes and survival of reoxygenation, we complemented the *NDA* null line *nda1-1*

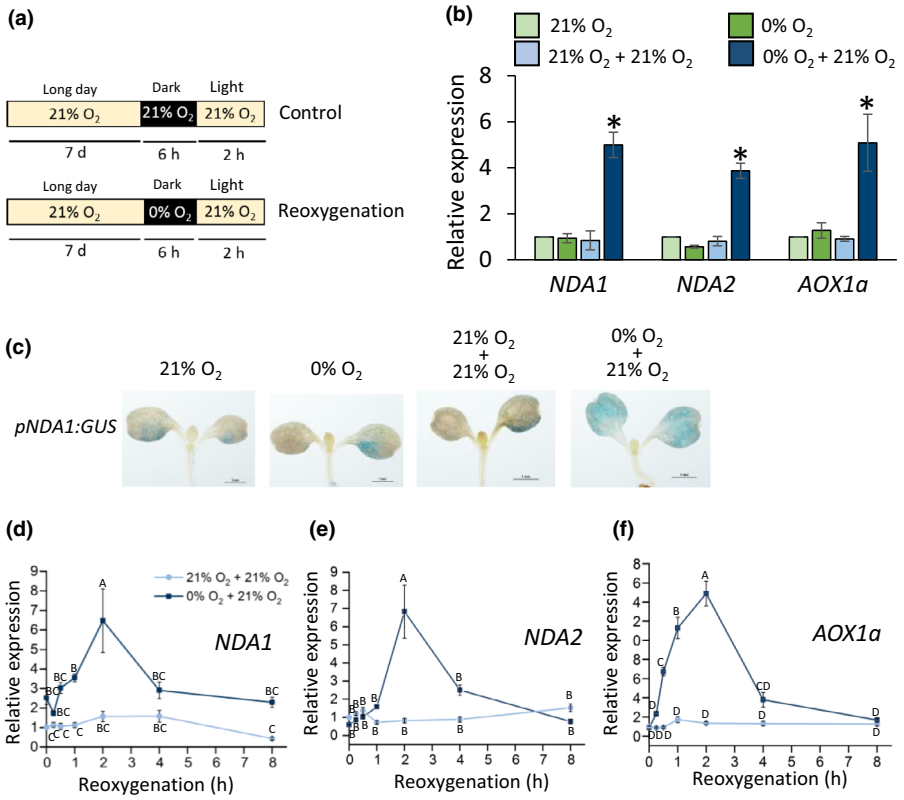

Fig. 2 The alternative mETC genes *NDA1*, *NDA2*, and *AOX1a* are induced by reoxygenation following anoxia. (a) Experimental scheme depicting anoxia and subsequent reoxygenation treatment. (b) Relative transcript levels measured by RT-qPCR in shoots of 7-d-old seedlings exposed to air (21% O_2) or anoxia (0% O_2) followed by exposure to 21% O_2 as indicated in (a). Means (±SE) obtained in four independent experiments with two technical repeats each (Mann–Whitney test; *, $P < 0.05$). (c) *pNDA1:GUS* staining activity in seedlings exposed to air (21% O_2) or anoxia (0% O_2) followed by exposure to 21% O_2 as indicated in (a). Bar, 1 mm. (d) Relative *NDA1*, (e) *NDA2*, and (f) *AOX1a* transcript levels in shoots of 7-d-old light-grown seedlings exposed to 21% O_2 or 0% O_2 for 6 h in the dark followed by a recovery phase in air for up to 8 h in the light. RT-qPCR results are means (±SE) of three independent biological experiments (two-way ANOVA with Tukey's test, $P < 0.05$). Different letters indicate statistically different groups.

nda2-2 with *NDA1* expressed either under its endogenous promoter (*pNDA1:NDA1*) or driven by the 35S promoter (*NDA1ox*) to achieve overexpression (Fig. S5). Reverse transcription-quantitative real-time PCR (RT-qPCR) analysis of *NDA1* expression and a survival assay revealed restoration of *NDA1* transcript levels and of seedling survival of reoxygenation to WT levels when *NDA1* was expressed under its endogenous promoter in *nda1-1 nda2-2 pNDA1:NDA1* plants, and elevated *NDA1* expression and improved survival in the overexpression lines *nda1-1 nda2-2 NDA1ox1* and *nda1-1 nda2-2 NDA1ox2* (Figs S5, S6). While cloning of the *NDA2* promoter was unsuccessful in our hands, overexpression of *NDA2* in the null background was achieved. The complementation lines *nda1-1 nda2-2 NDA2ox3* and *nda1-1 nda2-2 NDA2ox4* plants had elevated *NDA2* transcript levels and restored survival ability (Figs S5B,C, S6).

To assess whether the changes in *NDA* gene expression were also reflected in the NDA protein abundance in mitochondria, NDA1 and NDA2 proteins were analyzed in mitochondria isolated from WT, *NDA* knockout, and *NDA* overexpression lines using label-free quantitative mass spectrometry (Figs 1d, S7). NDA1 and NDA2 proteins were beyond the detection limit in *nda1-1 nda2-2*, whereas *NDA1ox3* contained NDA1 protein at mildly increased abundance as compared to WT. *NDA2ox2* contained elevated levels not only of NDA2 protein but also of NDA1 protein, suggesting a yet uncharacterized crosstalk in the expression of both proteins (Fig. 1d). The mass spectrometry analysis validated that the mitochondrial NDA proteins were absent in the double mutant and more abundant in the overexpression lines (Figs 1d, S3, S7). Taken together, the complementation and protein expression data provide confidence that survival of anoxia and reoxygenation is functionally linked to the NDAs and their role in mitochondrial alternative electron transport.

At the transcript level, *NDA1* and *NDA2* were induced by reoxygenation in shoots and roots but not by anoxia or a dark/light switch (Figs 2b, S8A,C). *AOX1a* was also upregulated during reoxygenation and not during anoxia (Fig. 2b). A time course analysis revealed transient induction of *NDA1*, *NDA2*, and *AOX1a* that peaked 2 h after reoxygenation (Fig. 2d–f). Elevated expression of *NDA1* after reoxygenation, and not during anoxia (0% O_2) or hypoxia (2% O_2), was independently confirmed using a *pNDA1:GUS* reporter line (Figs 2c, S8B).

NDA activity supports recovery of photosynthesis during reoxygenation

To explore how NDA proteins improve the survival of anoxia and reoxygenation in photosynthetically active tissues, we assessed the recovery of photosynthesis upon reoxygenation. NDA1 and NDA2 were required for the recovery of photosynthetic efficiency of photosystem II (PSII) as determined by the F_V/F_M ratio (Fig. 3a,b). *NDA1ox3* and *NDA2ox2* seedlings showed better PSII recovery than WT. F_V/F_M values increased from 0.56 at the end of the anoxic phase to *c.* 0.72 after 8 h of reoxygenation in *NDA* overexpressors compared with *c.* 0.63 in WT and 0.35 in *nda1-1 nda2-2* seedlings, indicating that activity

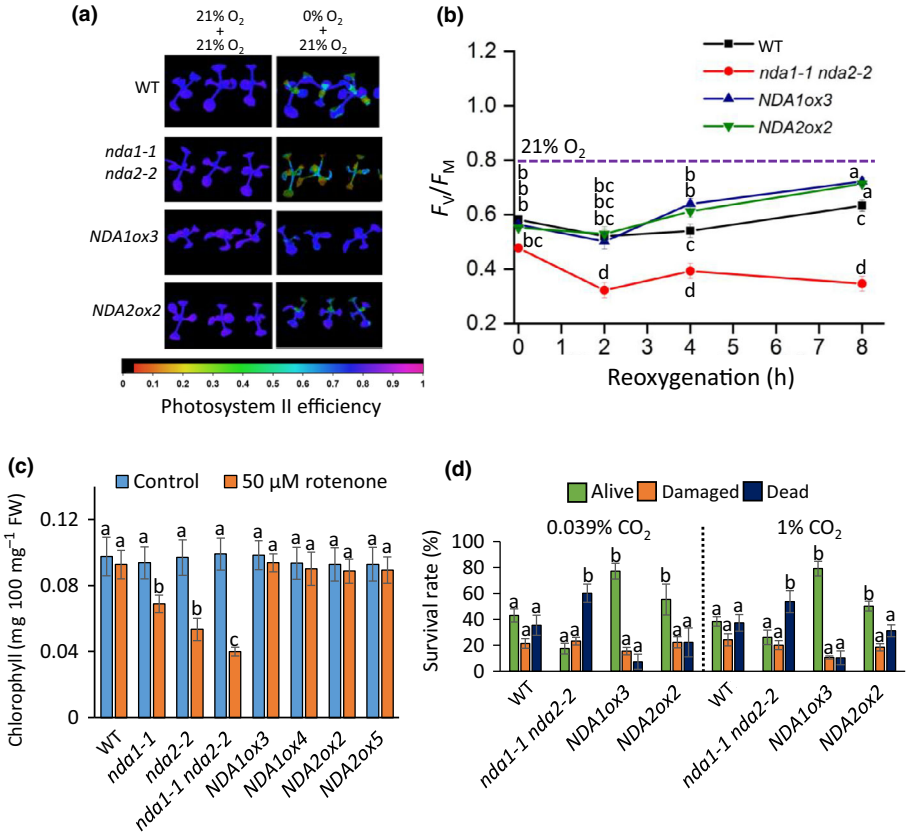

Fig. 3 *NDA1* and *NDA2* improve seedling survival of reoxygenation by protecting chloroplastic PSII. (a) The maximum quantum efficiency of photosystem II (F_V/F_M) of 11-d-old wild-type (WT), *nda1-1 nda2-2*, *NDA1ox3*, and *NDA2ox2* seedlings shown in false color. (b) Mean F_V/F_M values (±SE, $n = 30$–35, Kruskal–Wallis test, $P < 0.05$) obtained in three biological replicates. The purple line indicates the F_V/F_M value of the genotypes at normoxic oxygen conditions. (c) Seven-day-old WT and mutant seedlings were treated with 50 µM rotenone or left untreated and chlorophyll content was analyzed after 7 d of treatment (±SE, $n = 3$, Kruskal–Wallis test, $P < 0.05$). (d) Survival of 7-d-old WT, *nda1-1 nda2-2*, *NDA1ox3*, and *NDA2ox2* seedlings exposed to 16 h of 0% O_2 in the dark followed by 7 d of recovery under ambient air or air supplemented with 1% CO_2 (means ± SE, $n = 15$, obtained in three independent experiments, one-way ANOVA, $P < 0.05$). Different letters indicate statistically different groups.

of NDAs is essential for the recovery of photosynthetic activity following the anoxia–reoxygenation cycle. To further validate the functional link between mitochondrial NDA activity and chloroplast function, we inhibited the NADH oxidation capacity of mitochondrial complex I by exposing seedlings to rotenone for 7 d (Møller, 2001). This treatment did not alter chlorophyll content in WT or *NDA1* or *NAD2* overexpressors but resulted in decreased chlorophyll content in *nda1-1* and *nda2-2* seedlings and a reduction to less than half in *nda1-1 nda2-2* seedlings (Fig. 3c). These data indicate that NDA activity is essential to maintain functionality of photosynthetic electron transport in the chloroplast when mitochondrial NADH oxidation by complex I is limiting. Such a situation is particularly likely to occur at reoxygenation in the light.

To test whether photorespiration, which generates H_2O_2 at high rates in the peroxisomes and relies on the mETC as a high-capacity electron sink, plays a role in survival of the anoxia–reoxygenation cycle, we compared the survival of WT, *nda1-1 nda2-2*, *NDA1ox3*, and *NDA2ox2* seedlings that were exposed to either ambient air with 0.039% CO_2 during reoxygenation or to air supplemented with 1% CO_2 to prevent photorespiration (Fig. 3d). Survival rates did not differ between low and high CO_2 treatments in either WT, *nda1-1 nda2-2*, *NDA1ox3*, and *NDA2ox2* indicating that photorespiration is not a decisive factor in survival. Taken together, these results indicate that the NDA-mediated alternative mETC protects photosynthetic function in the chloroplast during reoxygenation in the light.

NDA1 is regulated by the transcription factors ANAC016 and ANAC017 that bind to the mitochondrial dysfunction motif in the *NDA1* promoter

Considering the similar induction profiles of the *NDA1* and *NDA2* transcripts upon reoxygenation, we focused on *NDA1* and aimed to identify the transcription factors controlling the observed upregulation. The *NDA1* promoter contains a mitochondrial dysfunction motif (MDM) 366–379 bp upstream of the transcription start site (Fig. 4a), which was previously identified as a binding site for ANAC transcription factors (De Clercq *et al.*, 2013). Of the large family of ANAC transcription factors, ANAC013, ANA0C016, and ANAC017 were associated with the response to mitochondrial dysfunction (De Clercq *et al.*, 2013; Van Aken *et al.*, 2016b). An EMSA showed selective binding of ANAC013, ANAC016, and most notably of ANAC017 to the MDM of the *NDA1* promoter (Fig. 4b). Consistently, we observed transactivation of the *NDA1* promoter by ANAC016 and ANAC017 in protoplasts using a luciferase reporter under the control of the 1055 bp *NDA1* promoter sequence with ANAC017 displaying strongest transactivation (Fig. 4c). The *NDA2* promoter lacks an MDM but has the consensus NAC protein binding site sequence (T/G)CGTGT (Tran *et al.*, 2004; Olsen *et al.*, 2005; Ng *et al.*, 2013; Fig. S9A). A 996 bp *NDA2* promoter sequence was not transactivated by ANAC013, ANAC016, or ANAC017 in accord with the lack of an MDM (Fig. S9B). We next analyzed *NDA1*, *NDA2*, and *AOX1a* expression in the loss-of-function mutants *anac016* and

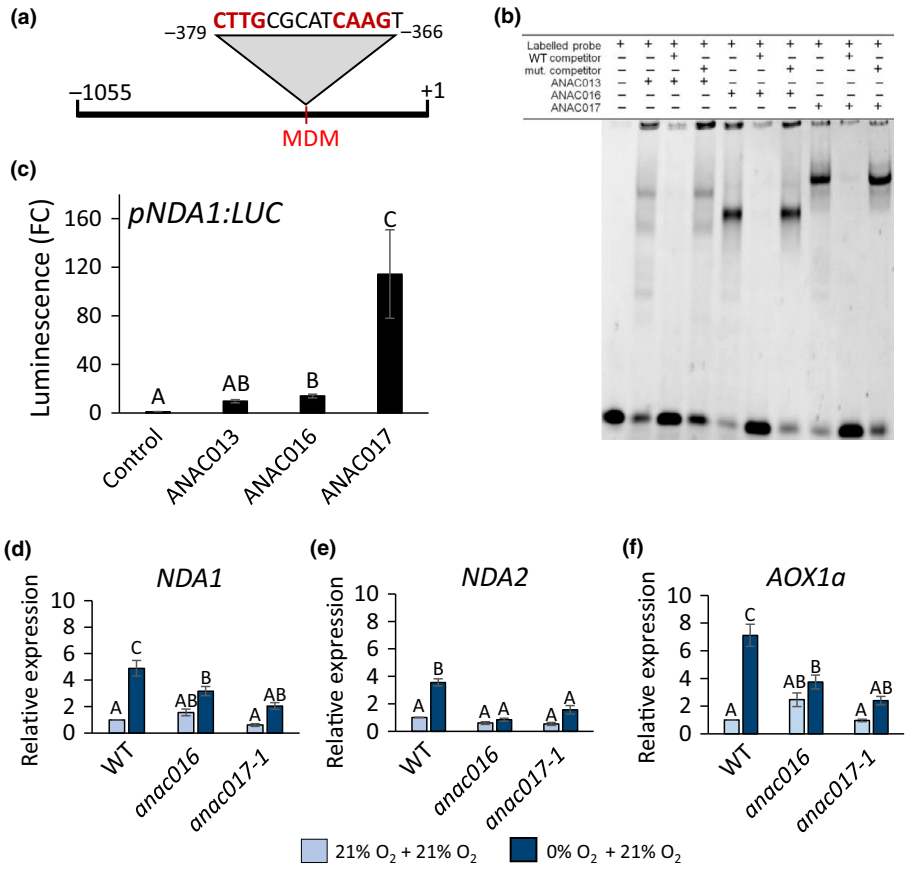

Fig. 4 ANAC016 and ANAC017 bind to and activate the *NDA1* promoter and are required for full induction of *NDAs* and *AOX1a* during reoxygenation. (a) Position of the mitochondrial dysfunction motif (MDM) in the *NDA1* promoter. The MDM consensus sequence is indicated by red letters. (b) Binding of ANAC013, ANAC016 and ANAC017 to the MDM motif in the *NDA1* promoter was analyzed by EMSA. IR-dye680-labeled MDM or mutated MDM from the *NDA1* promoter were incubated with FLAG-ANAC013, FLAG-ANAC016 or FLAG-ANAC017 and competition for binding was tested with unlabeled MDM probes. (c) Activation of the *NDA1* promoter by ANAC013, ANAC016, and ANAC017 analyzed by luciferase transactivation. *pNDA1:LUC* was co-transformed with *35S:ANAC013*, *35S:ANAC016* or *35S:ANAC017* into Arabidopsis shoot protoplasts. For normalization, *35S:RLUC* (Renilla luciferase) was co-expressed with each *35S:ANAC* vector. Results are means of four biological replicates ± SD (one-way ANOVA with Tukey's test, $P < 0.05$); FC, fold change. (d–f) Relative expression levels of *NDA1*, *NDA2*, and *AOX1a* in shoots of 7-d-old wild-type (WT), *anac016*, and *anac017-1* seedlings exposed to air (21% O_2) or anoxia (0% O_2) for 6 h in the dark followed by recovery in 21% O_2 for 2 h in the light. Results are means (±SE) of five independent biological replicates with two technical repeats each (two-way ANOVA with Tukey's test, $P < 0.05$). Different letters indicate statistically different groups.

anac017-1 (Kim *et al.*, 2013; Ng *et al.*, 2013), which we verified by RT-qPCR (Fig. S9C,D). At 21% O_2, transcript levels of *NDA1*, *NDA2*, and *AOX1a* were not significantly different between WT, *anac016*, and *anac017-1* (Fig. 4d–f). Reoxygenation induced *NDA1*, *NDA2*, and *AOX1a* transcripts to higher levels in the shoots of WT than in shoots of *anac016* and *anac017-1* seedlings (Fig. 4d–f), supporting the conclusion that the NDA-dependent alternative mETC is, at least in part, transcriptionally controlled by ANAC016 and ANAC017. Taking the findings of promoter binding and expression studies together, we conclude that *NDA1* expression is regulated by ANAC016 and ANAC017 through direct binding to the *NDA1* promoter, whereas *NDA2* regulation by ANAC016 and ANAC017 appears to be indirect.

We next assessed whether *ANAC013*, *ANAC016*, and *ANAC017* are regulated by reoxygenation (Fig. 5a–c). *ANAC013* transcripts increased within 30-min reoxygenation, peaked at 1 h, and declined to control levels after 4 h (Fig. 5a). *ANAC016* and *ANAC017* transcripts also increased albeit to a lesser extent (Fig. 5b,c). The rapid induction of *ANACs* suggests a function upstream of *NDA1* and *NDA2*. To test for a role of *ANAC016* and *ANAC017* in postanoxic stress alleviation, loss-of-function seedlings (Fig. S9C,D) were exposed to the anoxia/reoxygenation treatment. *anac016* and *anac017-1* seedlings showed reduced survival as compared to the WT (Fig. 5d) similar to the observations for the *nda1-1 nda2-2* seedlings (Fig. 1a). Notably, knockout of either *ANAC016* or *ANAC017* promoted shoot growth at unstressed conditions suggesting a similar trade-off between basal stress resistance and growth as seen with *nda1-1 nda2-2* and *NDAox* lines (Figs 1b, 5e). To test whether ANAC016 and ANAC017 mediate tolerance not only to the model treatment of anoxia/reoxygenation but also to transient submergence stress, we exposed soil-grown WT, *nda1-1 nda2-2*, *NDA1ox3*, *NDA2ox2*, *anac016*, and *anac017-1* plants to a submergence/desubmergence regime and scored survival following recovery (Fig. 5e,f). The survival rates resembled those observed with the anoxia/reoxygenation treatment. *anac016*, *anac017-1*, and *nda1-1 nda2-2* had higher mortality, and *NDA1ox3* and *NDA2ox2* had the same or

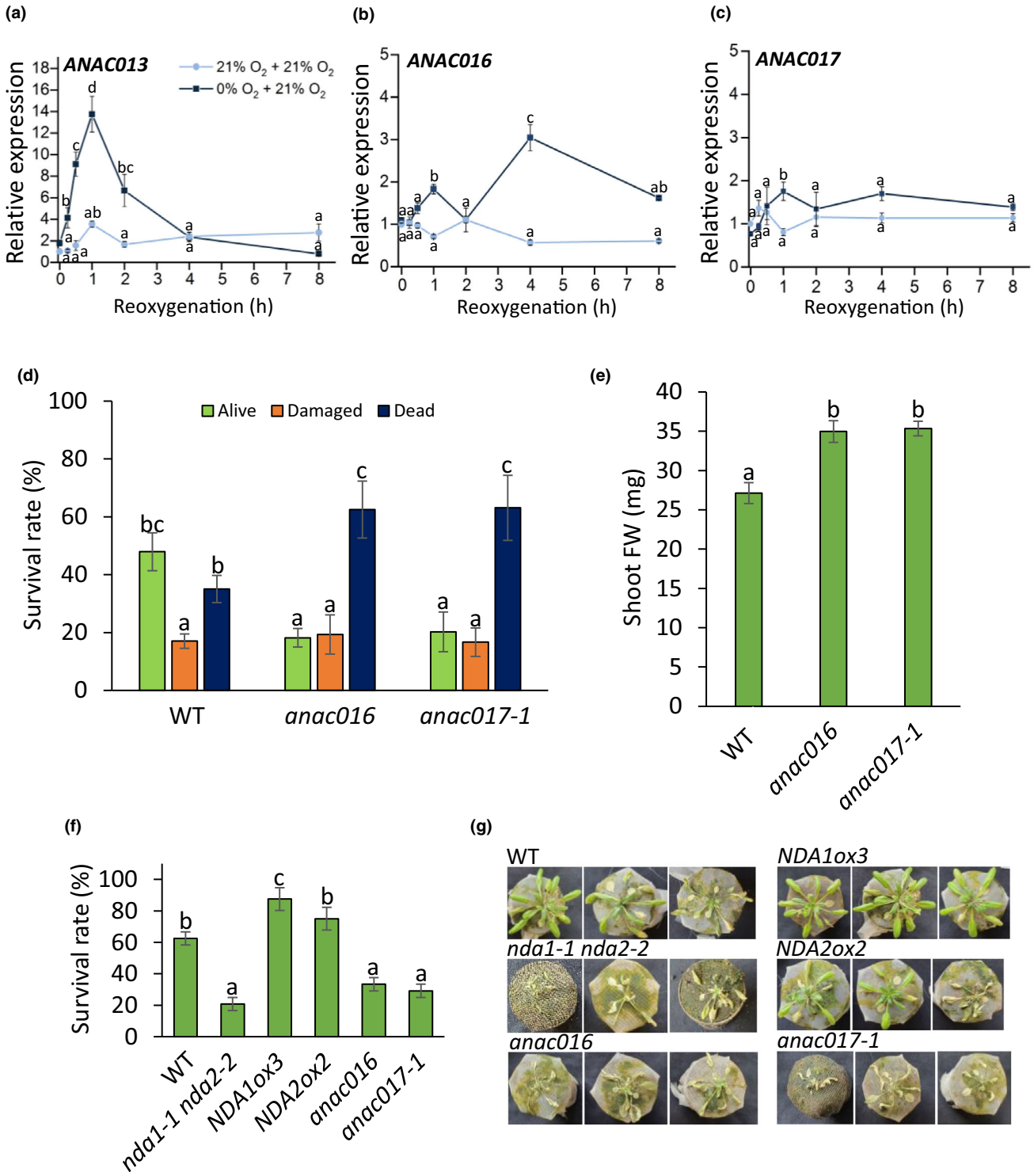

Fig. 5 *ANAC016* and *ANAC017* are crucial for seedling survival of reoxygenation and desubmergence. (a–c) Time course analysis of (a) *ANAC013* (b) *ANAC016*, and (c) *ANAC017* transcript levels determined by RT-qPCR in shoots of 7-d-old light-grown seedlings exposed to air or anoxia for 6 h in the dark followed by recovery in 21% O_2 in the light. Means (±SE) of three independent replicates with two technical repeats (two-way ANOVA with Tukey's test, $P < 0.05$). (d) Seven-day-old wild-type (WT), *anac016*, and *anac017-1* seedlings were exposed to 16 h of anoxia in the dark and then returned to long day. The percentage of alive, damaged, and dead seedlings was determined after 7 d of recovery. Results (±SE, $n = 12$, two-way ANOVA with Tukey's test, $P < 0.05$) obtained in three independent experiments. (e) Shoot fresh weight of 14-d-old seedlings grown in long day. Results are means (±SE, $n = 29$, one-way ANOVA with Tukey's test, $P < 0.05$) obtained in three independent experiments. (f) Four-wk-old WT, *nda1-1 nda2-2*, *NDA1ox3*, *NDA2ox2*, *anac016*, and *anac017-1* soil-grown plants were submerged for 3 d in the dark followed by desubmergence. The survival rate was determined after 7 d of recovery in long-day conditions and is shown as mean values (±SE, $n = 22–24$, one-way ANOVA with Tukey's test, $P < 0.05$) obtained in three independent experiments. Different letters indicate statistically different groups. (g) Representative plants after recovery.

lower mortality as WT, indicating that ANAC-regulated dissipation of reducing equivalents through NDAs is important for tolerating transient submergence.

NDA1 and *NDA2* do not alter the dynamics of NADH : NAD^+ and ATP during anoxia and reoxygenation

To better understand the physiological role of NDAs in reoxygenation, we analyzed the physiological dynamics of NAD redox status and $MgATP^{2-}$ levels, both of which are intimately linked to mETC activity and degree of respiratory coupling. To test whether NDA activity affects the NADH : NAD^+ ratio or $MgATP^{2-}$ levels in living tissue, we used *in vivo* biosensing and UPLC-based adenylate quantification. We stably expressed the NAD redox sensor Peredox-mCherry (Hung *et al.*, 2011) in the cytosol of WT, *nda1-1 nda2-2*, and *NDAox* lines for live monitoring of the cytosolic NADH : NAD^+ ratio during an anoxia–reoxygenation regime using multiwell plate reader fluorimetry (Wagner *et al.*, 2019; Steinbeck *et al.*, 2020; Fig. 6a). Wild-type, *nda1-1 nda2-2*, *NDA1ox3*, and *NDA2ox2* seedlings showed comparable NAD redox dynamics in response to changing oxygen concentrations (Fig. 6a). The NADH : NAD^+ ratio decreased within the first 2.5 h to a new steady state that is typically observed after moving tissue from the ambient light into darkness. Lowering of the oxygen concentration led to rapid NAD reduction which remained high over the hypoxic period and gradually decreased after reoxygenation (Fig. 6a). This finding is in line with limiting mETC and alternative mETC activities in the absence of molecular oxygen resulting in NADH accumulation not only in the mitochondrial matrix but also in the cytosol (both compartments are effectively connected *via* metabolic shuttle systems). To monitor ATP levels in live cells, the $MgATP^{2-}$ sensor ATeam 1.03 nD/nA (De Col *et al.*, 2017) was stably expressed in the cytosol of WT, *nda1-1 nda2-2* and *NDA1* and *NDA2* overexpression lines (Fig. 6b). In seedlings exposed to anoxia for 6 h, ATP levels rapidly and continuously declined in all genotypes. Upon reoxygenation, $MgATP^{2-}$ levels recovered rapidly and independently of genotype revealing robust and

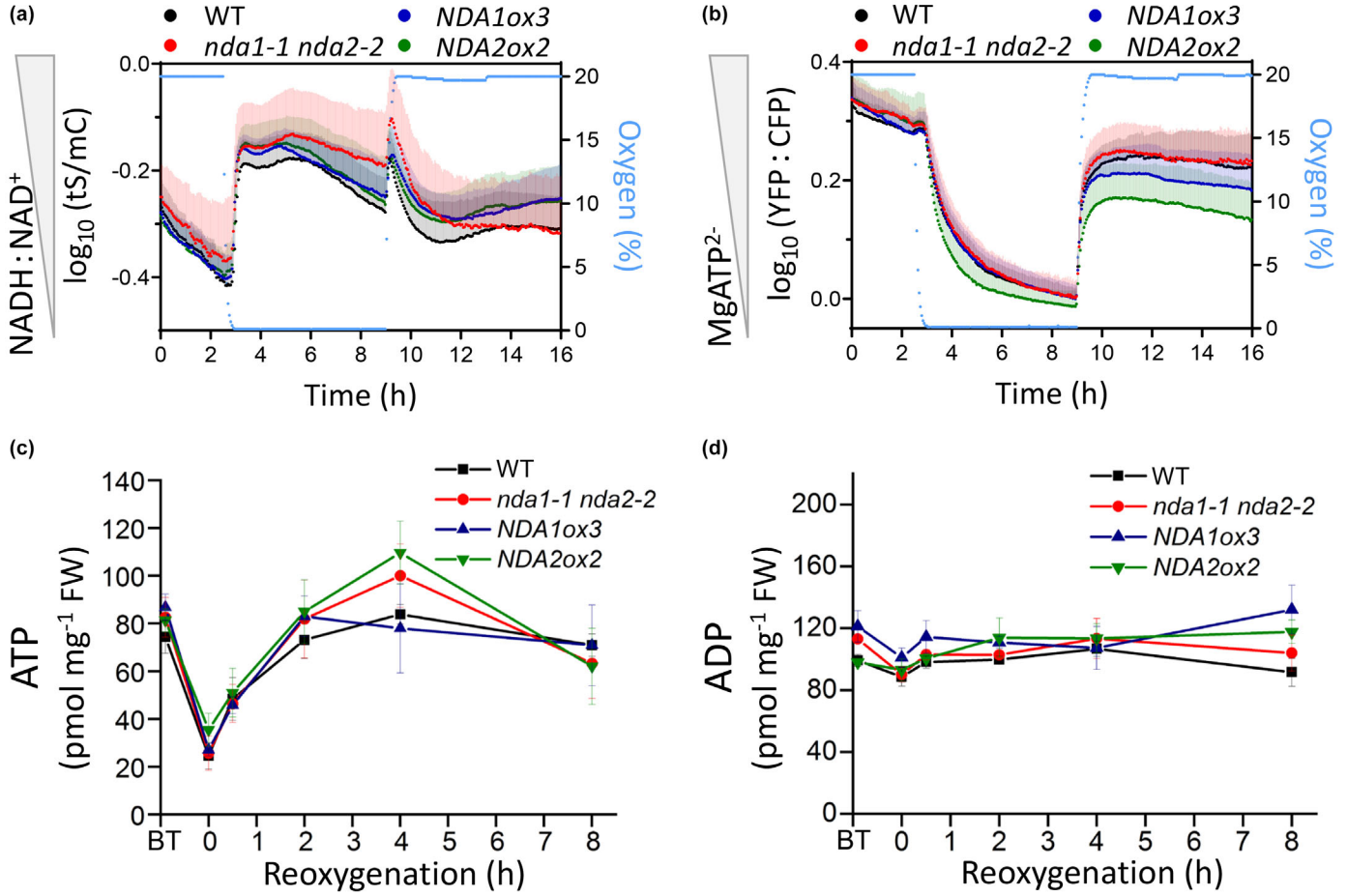

Fig. 6 NDA activity does not alter NAD redox balance or ATP levels. (a) Cytosolic NADH : NAD^+ was assessed by the Peredox-mCherry sensor stably expressed in wild-type (WT), *nda1-1 nda2-2*, *NDA1ox3*, and *NDA2ox2*. mC, mCherry fluorescence intensity; tS, tSapphire fluorescence intensity. (b) ATP assessed with the stably expressed ATeam 1.03 nD/nA sensor using multiwell plate reader-based fluorimetry. CFP, cyan fluorescent protein fluorescence intensity; YFP, yellow fluorescent protein fluorescence intensity. (a, b) Measurements were taken in 7-d-old seedlings (Means of $\log_{10}$-transformed fluorescence emission intensity ratios + SD as indicated by shading of corresponding colour, $n = 13$–16). (c) UPLC-based quantification of ATP. (d) UPLC-based quantification of ADP. (c, d) Measurements were taken in shoots of 7-d-old seedlings. Means (±SE) of four biological replicates. No significant differences were detected between genotypes (one-way ANOVA with Tukey's test, $P < 0.01$). BT, before treatment.

efficient postanoxic ATP production that was independent of mitochondrial NDA1 and NDA2 protein abundance (Figs 1d, 6b). Since the *in vivo* sensing analyses were only feasible in darkness, we used UPLC-based quantification of whole tissue ATP and ADP contents during reoxygenation of WT, *nda1-1 nda2-2*, *NDA1ox3*, and *NDA2ox2* seedlings in the light. Consistently, those measurements did not reveal any genotype-specific changes in ATP and ADP (Fig. 6c,d), indicating that cellular energy metabolism is sufficiently resilient to compensate for the loss of both NDAs during postanoxic stress and that there are other reasons why NDAs are required for protection from postanoxic stress.

NDA1 and NDA2 limit $O_2^{\bullet-}$ and H_2O_2 production during reoxygenation

Considering that low oxygen elevates the cytosolic NADH : NAD^+ ratio (Fig. 6a; Wagner *et al.*, 2019), which is linked to the reduction in the redox carriers of the mETC, reoxygenation may trigger the excessive formation of $O_2^{\bullet-}$, and in turn H_2O_2, by the mETC (Møller, 2001; Murphy, 2009). Since the alternative mETC can dissipate excess reductant from mETC components and NADH independent of the proton motive force across the inner mitochondrial membrane, we hypothesized that NDAs mitigate ROS formation during reoxygenation. To test this hypothesis, we analyzed the formation of $O_2^{\bullet-}$ by NBT staining in leaves of WT, *nda1-1 nda2-2*, *NDA1ox3*, and *NDA2ox2* (Fig. 7a). Visual inspection and subsequent signal quantification revealed elevated $O_2^{\bullet-}$ production in NDA-deficient seedlings as compared to WT and *NDAox* lines, and reduced $O_2^{\bullet-}$ production in *NDAox* lines as compared to WT and *nda1-1 nda2-2* (Fig. 7a). Similarly, H_2O_2 production, estimated by DAB staining, was inversely related to NDA protein abundance in mitochondria (Figs 1d, 7b). Since histochemical NBT and DAB staining can only serve as a qualitative estimate and do not provide temporal resolution, we performed a time course analysis of oxygen radical formation by EPR spectroscopy during reoxygenation (Fig. 7c). The detected oxygen radical amount at the end of the anoxia phase was higher in leaves of *nda1-1 nda2-2* seedlings than in WT or *NDAox* lines. Radical levels increased further within 2 h of reoxygenation in all genotypes and returned to low steady-state levels within 8 h after reoxygenation in WT and *NDAox* lines whereas recovery in *nda1-1 nda2-2* seedlings took 24 h, indicating that NDAs protect from elevated radical

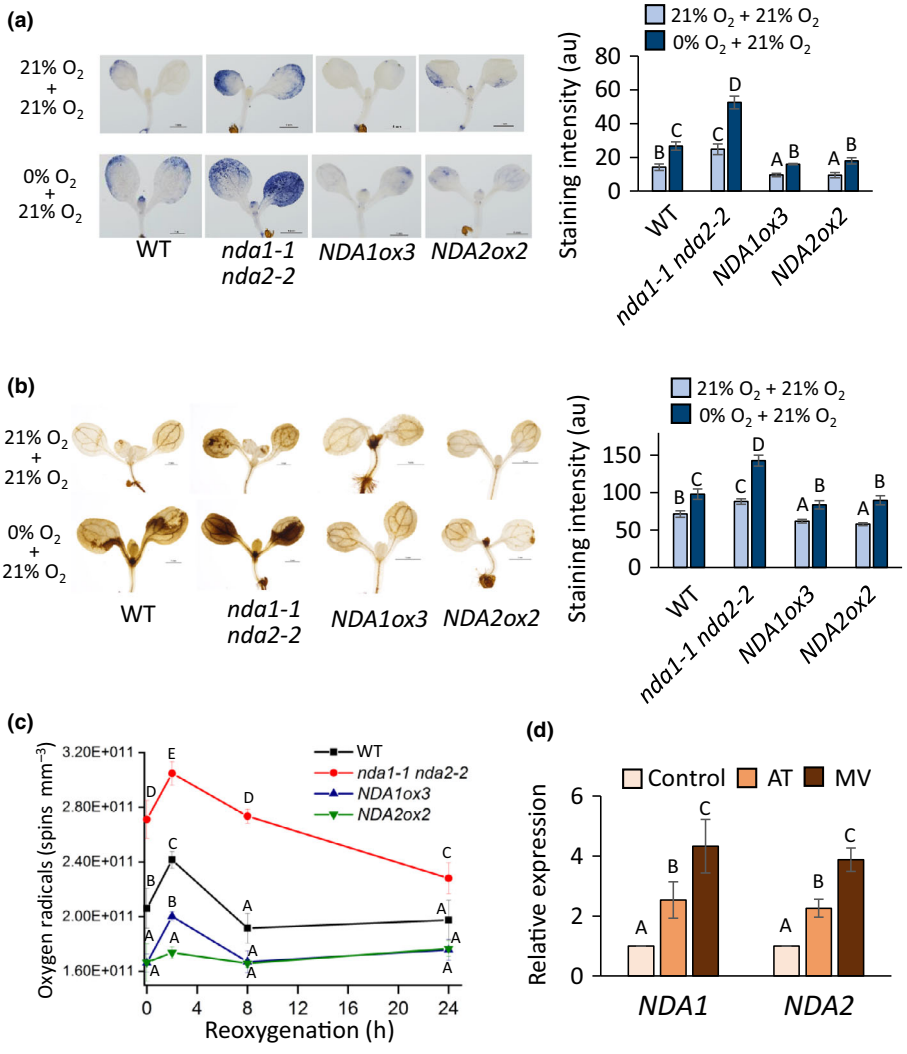

Fig. 7 *NDA1* and *NDA2* alter ROS homeostasis. (a) NBT staining of $O_2^{\bullet-}$ in representative 7-d-old wild-type (WT), *nda1-1 nda2-2*, *NDA1ox3*, and *NDA2ox2* seedlings exposed to 21% O_2 or 0% O_2 for 16 h in the dark followed by recovery in 21% O_2 for 2 h in the light. Bar, 1 mm. Quantification is given in arbitrary units (au) in the bar graph. (b) DAB staining of H_2O_2 in 7-d-old seedlings treated as in (a). Bar, 1 mm. (a, b) Quantified results are means (±SE, $n = 25$–32 seedlings, Kruskal–Wallis test, $P < 0.05$) determined in three independent experiments. (c) Time course analysis of oxygen radical species quantified by EPR spectroscopy in shoots of 7-d-old WT, *nda1-1 nda2-2*, *NDA1ox3*, and *NDA2ox2* seedlings exposed to 0% O_2 for 16 h in the dark followed by recovery in air for up to 24 h in the light. Results are means (±SE, one-way ANOVA with Tukey's test, $P < 0.05$) of three independent experiments. (d) Relative transcript levels of *NDA1* and *NDA2* were determined by RT-qPCR in shoots of 7-d-old seedlings treated with 3-amino-1,2,3-triazole (AT) or methyl viologen (MV) or left untreated for 3 h. Results are means (±SE, one-way ANOVA with Tukey's test, $P < 0.05$) of three independent biological experiments with two technical repeats each. Different letters indicate statistically different groups.

production during anoxia and efficiently limit radical formation following reoxygenation (Fig. 7c). To test whether mitochondria, where NDA-dependent mETC takes place, are major sites of ROS formation in response to changing O_2, we performed mitochondria-specific assessment of H_2O_2 dynamics. We employed Arabidopsis lines expressing the genetically encoded biosensor roGFP2-Orp1 either in the mitochondrial matrix or in the cytosol to monitor the specific *in vivo* H_2O_2 dynamics in either compartment (Nietzel *et al.*, 2019; Figs 8, S10). *In vivo* sensor functionality and responsiveness were validated by driving the sensor to full reduction or oxidation, respectively (Fig. S10). Multiwell plate reader-based monitoring of seedlings exposed to changing O_2 as introduced previously (De Col *et al.*, 2017; Wagner *et al.*, 2019; Ugalde *et al.*, 2022) revealed reduction in the sensor in the first hour of the near-anoxia treatment (set to 0.1% O_2), indicating H_2O_2 production at lower rates. This phase was followed by a steady increase of sensor oxidation indicating elevated rates of H_2O_2 production or lower rates of H_2O_2 scavenging under near-anoxia. The oxidation was more pronounced in mitochondria than in the cytosol (Fig. 8a–c). At reoxygenation, a transient burst in oxidation occurred in both compartments, indicating a sudden release of H_2O_2 at high rate, before the sensor oxidation recovered toward a new steady state within 2–3 h. The ROS burst showed a higher amplitude and lasted for longer in mitochondria than in the cytosol (Fig. 8d,e). The observation that mitochondrial H_2O_2 dynamics show a more pronounced increase during the O_2 regime supports the finding that NDA abundance in mitochondria impacts on cellular ROS dynamics with elevated ROS production in *nda1-1 nda2-2* and reduced ROS in *NDAox* lines than WT (Fig. 7c, 0 h). A direct comparison of subcellular H_2O_2 dynamics between the different NDA genotypes could not be performed due to pronounced biosensor silencing in all transgenic backgrounds and deserves future establishment. Data from the three approaches taken together reveal that mitochondria are a major source of ROS in a low-oxygen environment and during reoxygenation and that NDA proteins limit ROS formation.

NDAs are induced by ROS-associated inhibitors

Mitochondrial ROS production has been suggested as an upstream signal of ANAC-mediated retrograde signaling (De Clercq *et al.*, 2013; Ng *et al.*, 2013). Considering that *NDA1* expression is controlled by ANAC016 and ANAC017 (Fig. 4), we hypothesized that ROS formed at reoxygenation may serve as a signal for *NDA* regulation. The catalase inhibitor 3-amino-1,2,3-triazole (AT) that impairs efficient intracellular H_2O_2 removal by the peroxisomes (Amory *et al.*, 1992; Prasad *et al.*, 1994) induced expression of *NDA1* and *NDA2* as did methyl viologen (MV) that promotes $O_2^{\bullet-}$ formation in

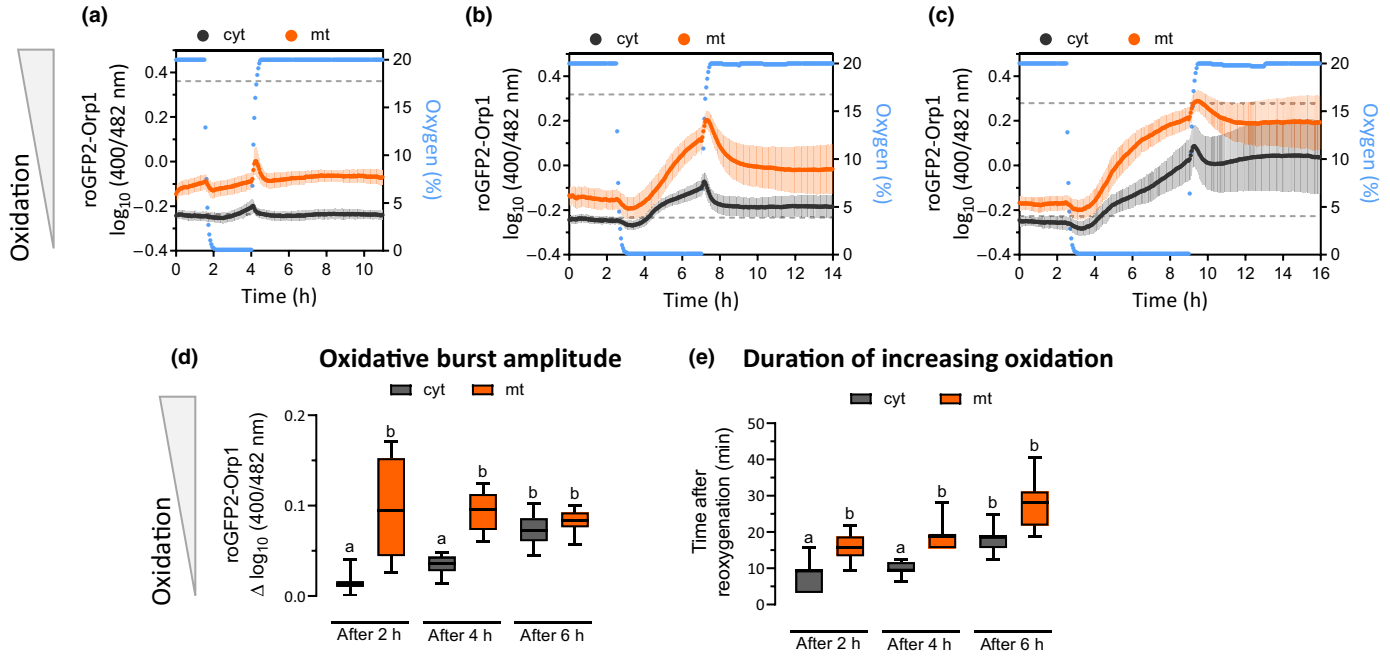

Fig. 8 Reactive oxygen species production measured with the roGFP2-Orp1 biosensor in the cytosol and mitochondria under changing O_2 conditions. Cytosolic (cyt) and mitochondrial (mt) H_2O_2 was assessed with the roGFP2-Orp1 sensor stably expressed in cytosol or mitochondria using multiwell plate reader-based fluorimetry in seedlings exposed to (a) 2 h anoxia, (b) 4 h anoxia, and (c) 6 h anoxia of 0.1% O_2 followed by reoxygenation. Dashed lines indicate the upper and lower detection limits of the roGFP2-Orp1 sensor determined for each line at the end of the treatment (shown in Supporting Information Fig. S10) (a–c: means of $\log_{10}$-transformed fluorescence intensity excitation ratios ± SD as indicated by shading of corresponding colour, $n = 11$–16). (d) The cytosolic and mitochondrial oxidative burst amplitude was calculated by subtracting $\log_{10}$-transformed ratio of the respective roGFP2-Orp1 sensor after 2, 4, and 6 h of anoxia from the maximum ratio reached after reoxygenation ($n = 12$–16, Kruskal–Wallis test, $P < 0.02$). (e) The duration until the maximum oxidation reached after 2, 4, and 6 h of anoxia ($n = 12$–16, Kruskal–Wallis test, $P < 0.005$). Different letters indicate statistically different groups. Boxes: 25th–75th percentile; the median is indicated by a horizontal line; whiskers: 5th–95th percentile.

chloroplasts and mitochondria (Cui *et al.*, 2019; Fig. 7d) suggesting that *NDA* expression may be regulated by intracellular ROS. Considering that mitochondria are a major site of ROS production during anoxia and reoxygenation and that ROS levels inversely correlate with mitochondrial NDA abundance, a central role of mitochondria in cellular ROS homeostasis under fluctuating O_2 availability appears likely.

Discussion

NDAs are crucial for ROS containment and survival during reoxygenation

In recent years, research on submergence tolerance has mostly centered on the submergence phase while desubmergence, marked by a surge in oxygen and light exposure, has received less attention. During desubmergence, plants acclimated to low oxygen are exposed to air resulting in excessive ROS formation that provides a cellular challenge that is distinct from the initial oxygen deficiency (Elstner & Osswald, 1994; Smirnoff, 1995; Van Aken *et al.*, 2016b). Despite several studies on reoxygenation in rice and Arabidopsis (Fukao *et al.*, 2011; Tsai *et al.*, 2014, 2016; Yuan *et al.*, 2017; Yeung *et al.*, 2018; Meng *et al.*, 2020), the molecular and cellular mechanisms that regulate reoxygenation stress tolerance are not fully understood. In this study, we mimicked submergence/desubmergence by applying a dark-anoxia/light-normoxia regime and focused on the reoxygenation phase.

Our data indicate that electron removal *via* the alternative mETC components NDA1 and NDA2 protects from excess ROS formation (Fig. 7). On the one hand, ROS are signaling molecules that help plants to sense their environment and trigger adaptive responses (Bailey-Serres *et al.*, 2012; Devireddy *et al.*, 2021). During hypoxia, H_2O_2 controls the expression of alcohol dehydrogenase (ADH), and ADH activity is modified by Cys oxidation *in vitro* to underpin energy supply *via* fermentation (Yang, 2014; Dumont *et al.*, 2018). On the other hand, ROS are reactive. They can cause irreversible oxidative damage to lipids, proteins, and nucleic acids, and even trigger programmed cell death (Møller *et al.*, 2007; Pérez-Pérez *et al.*, 2012). Therefore, plants need to balance ROS formation with ROS scavenging to survive reoxygenation (Yeung *et al.*, 2019). The flood-tolerant Arabidopsis accession Lp2-6 showed restricted ROS accumulation during the first hour of reoxygenation, and improved survival of reoxygenation suggesting that tolerance to reoxygenation correlates with controlled ROS accumulation during the early recovery phase (Yeung *et al.*, 2018). By contrast, the flood-sensitive Bay-0 accession was less efficient in controlling ROS during reoxygenation and showed reduced survival (Yeung *et al.*, 2018). Arabidopsis seedlings overexpressing the transcription factor gene *MYC2* showed efficient control of ROS and increased survival during reoxygenation compared with the *myc2-2* knockout mutant that displayed excessive ROS production and reduced survival (Yuan *et al.*, 2017). Transcript levels of genes encoding the antioxidant enzymes ascorbate peroxidase 2 (APX2) and glutathione reductase 1 (GR1) were induced in Arabidopsis within 3 h of reoxygenation (Yuan *et al.*, 2017). In accord with the idea that survival of reoxygenation requires fine-balancing of ROS, the plasma membrane-localized respiratory burst oxidase homologue (RBOH) D, which generates $O_2^{\bullet-}$ in the extracellular space, was implicated in providing tolerance to reoxygenation stress in Arabidopsis (Yeung *et al.*, 2018). Here, we show that mitochondria are important sites of H_2O_2 formation when environmental O_2 concentrations change and that the NDA-dependent alternative mETC is instrumental in limiting cellular ROS during reoxygenation (Figs 7, 8). Taken together, an intricate network of ROS producing, preventing, and scavenging systems is in place to optimize cellular ROS levels under reoxygenation stress and failure of any part tips plant fate toward death. Reactive oxygen species formation and scavenging occur in different cellular compartments raising the question of how the rescue systems are coordinated. While evidence for ROS formation and induction of antioxidant defense responses during reoxygenation has been accumulating, few studies have been dedicated to understand the underlying regulatory mechanisms so far (Fukao *et al.*, 2011; Tsai *et al.*, 2014; Yuan *et al.*, 2017; Yeung *et al.*, 2018; Meng *et al.*, 2020). It deserves emphasizing that increased ROS production by partial reduction in molecular oxygen in cells is only plausible when residual amounts of oxygen are still available and cannot occur in the total absence of oxygen (Sasidharan *et al.*, 2017; Wagner *et al.*, 2018; Pucciariello & Perata, 2021).

NDAs are controlled by transcription factors that act in mitochondrial retrograde signaling

The expression levels of *NDA1*, *NDA2*, and *AOX1*a were significantly increased during reoxygenation (Fig. 2). Similarly, the alternative mETC components AOX and NDA were induced at the protein and transcript levels in rice seedlings during the reoxygenation phase following anoxia (Millar *et al.*, 2004; Narsai *et al.*, 2009). Reoxygenated rice coleoptiles were able to respire in the absence of complex IV due to the induction of AOX protein (Millar *et al.*, 2004), and overexpression of *AOX* in *Nicotiana tabacum* was shown to reduce nitro-oxidative stress during reoxygenation (Jayawardhane *et al.*, 2020). In addition, the activity of an *Aspergillus niger* alternative dehydrogenase was induced under oxidative stress in oxygen-enriched cultures of the fungus (O'Donnell *et al.*, 2011), a setup that mimics reoxygenation in plants. Increased expression of *NDA1* and *NDA2* when H_2O_2 removal is impaired (Amory *et al.*, 1992; Prasad *et al.*, 1994) and in response to increased chloroplastic ROS production, as well as induction of *AOX* isoforms by H_2O_2 or antimycin A (Vanlerberghe & McLntosh, 1996; Zarkovic *et al.*, 2005; Ng *et al.*, 2013) make it likely that ROS signaling contributes to the regulation of gene expression of alternative mETC components (Elstner & Osswald, 1994; Smirnoff, 1995; Huang *et al.*, 2016).

ANACs are plant-specific transcription factors involved in the response to oxidative stress and mitochondrial dysfunction (De Clercq *et al.*, 2013; Van Aken *et al.*, 2016b; Meng *et al.*, 2019, 2020; Shapiguzov *et al.*, 2019b; Mittler *et al.*, 2022). *NDA1* is recognized and activated by ANAC016 and ANAC017, and

anac016 and *anac017-1* seedlings show reduced induction of *NDA1* and *NDA2* during reoxygenation (Figs 4, 5). More so, overexpression of *ANAC017* increased *NDA1* transcript abundance (Meng *et al.*, 2019). *AOX1a* expression induced by ANAC017 provides protection from thiol-based reductive stress indicating adjustment of mitochondrial respiratory capacity *via* ANAC017-mediated retrograde signaling (Fuchs *et al.*, 2022). The *NDA2* promoter lacks an MDM site and is not activated by ANAC013, ANAC016, or ANAC017 (Fig. S8). ANAC017, ANAC055, and ANAC072 bind to an ANAC binding site in the *NDA2* promoter (Tran *et al.*, 2004; Olsen *et al.*, 2005; Ng *et al.*, 2013), but the specific hierarchy of transcriptional regulation of *NDA2* remains unresolved.

ANAC017 overexpression upregulates *ANAC013*, *ANAC016*, and *ANAC053* through a positive feedback loop suggesting that ANAC017 acts as a key regulator of mitochondrial retrograde signaling that impacts *NDA2* expression indirectly within this transcription factor network (De Clercq *et al.*, 2013; Meng *et al.*, 2019; Broda *et al.*, 2021; Fuchs *et al.*, 2022). Decreased survival of reoxygenation and desubmergence of *anac016* and *anac017-1* seedlings compared with WT reveals the importance of mitochondrial retrograde signaling *via* *ANAC016* and *ANAC017* in submergence/desubmergence tolerance (Bui *et al.*, 2020; Meng *et al.*, 2020).

ANACs are membrane-associated transcription factors that are attached to the endoplasmic reticulum. Under various stresses, they are released *via* proteolysis and translocate to the nucleus to initiate transcriptional responses (Kim *et al.*, 2006; Seo *et al.*, 2008; De Clercq *et al.*, 2013; Ng *et al.*, 2013; Van Aken *et al.*, 2016b). Since ROS have been long-term candidates to be involved in mitochondrial retrograde signaling (Murphy, 2009; Møller & Sweetlove, 2010; Crawford *et al.*, 2018), the ROS burst observed in mitochondria and, to a lesser extent, the cytosol during reoxygenation, might act as signal that initiates cleavage of ANAC017 to allow translocation to the nucleus to induce the expression of *NDA1* and *AOX1a*. Reactive oxygen species-mediated signaling in response to mitochondrial dysfunction and MV as stimulant for organellar $O_2^{\bullet-}$ production has been suggested previously (Ng *et al.*, 2014; Van Aken *et al.*, 2016a; Wang *et al.*, 2018; Ugalde *et al.*, 2021). Inhibition of complex III, which may elevate the rate of mitochondrial $O_2^{\bullet-}$ release (amongst various other cell physiological changes), was shown to initiate the cleavage of ANAC017 by a rhomboid protease in the ER membrane which in turn induced expression of mitochondrial dysfunction stimulon (MDS) genes including *AOX1a* (Ng *et al.*, 2013).

Alternative respiratory electron transport in the mitochondrion protects from photosystem II damage in the chloroplast during reoxygenation

The acclimation of the shoot to reoxygenation is strongly influenced by photosynthetic recovery. It is essential to prevent leaf senescence and cell death during reoxygenation (Kato *et al.*, 2014). In many plant species, a significant reduction in maximal quantum yield of PSII (F_V/F_M) and nonphotochemical quenching (NPQ) was observed during reoxygenation (Luo *et al.*, 2009, 2010, 2018; Sone & Sakagami, 2017). We observed PSII recovery in WT and *NDA* overexpressors, but not in *nda1-1 nda2-2*, revealing an essential role of the NDA-mediated alternative mETC in PSII rescue (Fig. 3). The submergence-sensitive Arabidopsis accession Bay-0 exhibited a lower F_V/F_M ratio than the submergence-tolerant accession Lp2-6 3 d after reoxygenation (Yeung *et al.*, 2018). Furthermore, the submergence-tolerant rice accession M202 (Sub1A) displayed unaltered non-photochemical quenching (NPQ) at the time of desubmergence as compared to non-submerged controls, while the submergence-sensitive M202 background showed strongly reduced NPQ (Alpuerto *et al.*, 2016) suggesting that maintaining efficient photosynthesis at desubmergence of shoot tissues is an important element of flooding tolerance. *NDA1* and *AOX1* are light-responsive and are further regulated diurnally pointing to a functional link between the alternative mETC and photosynthetic activity also beyond oxygen stress (Svensson & Rasmusson, 2001; Escobar *et al.*, 2004; Elhafez *et al.*, 2006; Rasmusson & Escobar, 2007). A role for respiration in optimizing the chloroplastic energy pool to maintain cellular carbohydrate levels is well-established (Vanlerberghe *et al.*, 2020). Maintaining this balance may plausibly become particularly important during stress when the formation of ROS in both mitochondria and chloroplasts can increase dramatically. Chloroplastic ROS metabolism of Arabidopsis is controlled by the nuclear-encoded MDS genes, one of which encodes for AOX1a (Shapiguzov *et al.*, 2019a). The alternative mETC prevents photoinhibition of PSII under high light and helps oxidize excess NADH (Yamada *et al.*, 2020). If not controlled, excessive ROS production, as a result of excess light, inactivates the reaction centers of PSI and PSII (Pospíšil, 2009). Photorespiration can dissipate a surplus in photochemical energy and prevent photo-oxidative damage (Kozaki & Takeba, 1996). Yet, our data suggest that seedling survival of reoxygenation was independent of photorespiratory activity.

Insufficient replenishment of energy reserves and redox imbalance impede plant survival during low-oxygen conditions and reoxygenation. Suppression of *NDA1* or *NDA2* affects the NAD(P)H redox balance (Wallström *et al.*, 2014). However, *in planta* fluorimetry and ultra-performance liquid chromatography (UPLC)-based quantification of ATP and ADP showed no differences in these metabolites between WT, *nda1-1 nda2-2*, *NDA1ox3*, and *NDA2ox2*. A very rapid increase in NADH : NAD^+ and a decrease in ATP levels were observed upon the onset of anoxia, but these were independent of NDA abundance (Fig. 6). Similarly, previous work on leaves of mature Arabidopsis rosettes exposed to a gradual hypoxia-anoxia treatment showed a decrease in ATP concentration and a rapid increase in the NADH : NAD^+ ratio (Wagner *et al.*, 2019). Likewise, Arabidopsis seedlings exposed to 4 h of anoxia showed a decrease in ATP levels (Tsai *et al.*, 2016). In this study, the NADH : NAD^+ ratio required several hours after reoxygenation for recovery, while ATP recovered faster, within 1 h (Tsai *et al.*, 2016). Quick recovery of NADH redox balance and ATP indicated that seedlings were able to effectively manage their energy and NADH redox balance independently of the presence and abundance of the

NDA proteins. The peroxide sensor roGFP2-Orp1 targeted to cytosol and mitochondria revealed a more pronounced and longer-lasting oxidative burst in mitochondria than in the cytosol revealing distinct subcellular peroxide accumulation during reoxygenation with mitochondria as a major site of intracellular ROS formation. The overall temporal dynamics of cytosolic peroxide production validate those observed recently (Liu *et al.*, 2022). The concomitant induction of *NDAs* by mitochondrial dysfunction signaling *via* ANAC transcription factors supports a specific role for mitochondrial ROS management in reoxygenation stress resistance.

The drastically impaired survival phenotype of the *nda1-1 nda2-2* line could result from any phase of the applied stress regimes of anoxia–reoxygenation or submergence–desubmergence. The phenotypic analysis of *nda1-1 nda2-2* alone is too crude to pinpoint when exactly NDA capacity is required for survival, since the double mutant is defective in both expression of the basal levels of the protein and induction of NDA expression at reoxygenation. Yet, the observation that the mutant lines *anac16* and *anac017-1*, which are not defective in the basal expression of *NDA1* and *NDA2* but impaired in their induction (Fig. 4d,e), show a similar survival phenotype as the *nda1-1 nda2-2* line (Figs 1a, 5d) provides a strong argument for the critical phase for survival occurring after the initial reoxygenation stress, that is, later during recovery when *NDA* expression is induced.

In conclusion, the alternative mETC with the internal alternative dehydrogenases NDA1 and NDA2 is a crucial pathway to prevent excessive ROS formation in mitochondria during reoxygenation. Electron transfer by NDAs in mitochondria reduces cellular ROS load, protects the photosynthetic machinery in the chloroplasts from oxidative damage, and thereby promotes photosynthetic recovery and plant survival. Our study provides direct evidence for the role of mitochondria as a hub of defense against reoxygenation stress.

Acknowledgements

The authors thank Timo Staffel (Plant Developmental Biology and Physiology, University Kiel) for excellent technical support. Open Access funding enabled and organized by Projekt DEAL.

Competing interests

None declared.

Author contributions

JJ and M Sauter designed the study and JJ performed major experiments and analyses. SL, RS-S, GP and JE performed specific experiments and the corresponding data analysis. M Schwarzländer, AS-H, MW, JTD, IF and WB assisted in designing the experiments and in interpreting the data from specific experiments. M Sauter and JJ wrote the manuscript with contributions from M Schwarzländer and SL.

ORCID

Wolfgang Bilger https://orcid.org/0000-0001-7800-4210
Joost T. Dongen van https://orcid.org/0000-0001-7944-9289
Jürgen Eirich https://orcid.org/0000-0003-0963-1872
Iris Finkemeier https://orcid.org/0000-0002-8972-4026
Jay Jethva https://orcid.org/0000-0002-3223-3488
Sophie Lichtenauer https://orcid.org/0000-0003-4525-6555
Gernot Poschet https://orcid.org/0000-0002-5344-0865
Margret Sauter https://orcid.org/0000-0002-7370-643X
Romy Schmidt-Schippers https://orcid.org/0000-0002-3395-0673
Markus Schwarzländer https://orcid.org/0000-0003-0796-8308
Anja Steffen-Heins https://orcid.org/0000-0002-5170-2155
Markus Wirtz https://orcid.org/0000-0001-7790-4022

Data availability

The raw data of the specific experiments based on which the figures were generated are available from Jay Jethva upon request. The full raw proteomic dataset can be accessed at: https://repository.jpostdb.org/entry/JPST001501.0.

References

Alpuerto JB, Hussain RMF, Fukao T. 2016. The key regulator of submergence tolerance, SUB1A, promotes photosynthetic and metabolic recovery from submergence damage in rice leaves. *Plant, Cell & Environment* **39**: 672–684.

Amory AM, Ford L, Pammenter NW, Cresswell CF. 1992. The use of 3-amino-1,2,4-triazole to investigate the short-term effects of oxygen toxicity on carbon assimilation by *Pisum sativum* seedlings. *Plant, Cell & Environment* **15**: 655–663.

Bailey-Serres J, Lee SC, Brinton E. 2012. Waterproofing crops: effective flooding survival strategies. *Plant Physiology* **160**: 1698–1709.

Biemelt S, Keetman U, Albrecht G. 1998. Re-aeration following hypoxia or anoxia leads to activation of the antioxidative defense system in roots of wheat seedlings. *Plant Physiology* **116**: 651–658.

Blokhina OB, Virolainen E, Fagerstedt KV, Hoikkala A, Wähälä K, Chirkova TV. 2000. Antioxidant status of anoxia-tolerant and -intolerant plant species under anoxia and reaeration. *Physiologia Plantarum* **109**: 396–403.

Broda M, Khan K, O'Leary B, Pružinská A, Lee CP, Millar AH, Van Aken O. 2021. Increased expression of ANAC017 primes for accelerated senescence. *Plant Physiology* **186**: 2205–2221.

Bui LT, Shukla V, Giorgi FM, Trivellini A, Perata P, Licausi F, Giuntoli B. 2020. Differential submergence tolerance between juvenile and adult Arabidopsis plants involves the ANAC017 transcription factor. *The Plant Journal* **104**: 979–994.

Camacho A, Moreno-Sanchez R, Bernal-Lugo I. 2004. Control of superoxide production in mitochondria from maize mesocotyls. *FEBS Letters* **570**: 52–56.

Clough SJ, Bent AF. 1998. Floral dip: a simplified method for *Agrobacterium*-mediated transformation of *Arabidopsis thaliana*. *The Plant Journal* **16**: 735–743.

Crawford T, Lehotai N, Strand Å. 2018. The role of retrograde signals during plant stress responses. *Journal of Experimental Botany* **69**: 2783–2795.

Cui F, Brosché M, Shapiguzov A, He X-Q, Vainonen JP, Leppälä J, Trotta A, Kangasjärvi S, Salojärvi J, Kangasjärvi J *et al.* 2019. Interaction of methyl viologen-induced chloroplast and mitochondrial signaling in Arabidopsis. *Free Radical Biology and Medicine* **134**: 555–566.

Cvetkovska M, Vanlerberghe GC. 2013. Alternative oxidase impacts the plant response to biotic stress by influencing the mitochondrial generation of reactive oxygen species. *Plant, Cell & Environment* **36**: 721–732.

Dahal K, Vanlerberghe GC. 2017. Alternative oxidase respiration maintains both mitochondrial and chloroplast function during drought. *New Phytologist* **213**: 560–571.

De Clercq I, Vermeirssen V, Van Aken O, Vandepoele K, Murcha MW, Law SR, Inzé A, Ng S, Ivanova A, Rombaut D *et al.* 2013. The membrane-bound NAC transcription factor ANAC013 functions in mitochondrial retrograde regulation of the oxidative stress response in *Arabidopsis thaliana*. *Plant Cell* **25**: 3472–3490.

De Col V, Fuchs P, Nietzel T, Elsässer M, Voon CP, Candeo A, Seeliger I, Fricker MD, Grefen C, Møller IM *et al.* 2017. ATP sensing in living plant cells reveals tissue gradients and stress dynamics of energy physiology. *eLife* **6**: e26770.

Devireddy AR, Zandalinas SI, Fichman Y, Mittler R. 2021. Integration of reactive oxygen species and hormone signaling during abiotic stress. *The Plant Journal* **105**: 459–476.

Dumont S, Bykova NV, Khaou A, Besserour Y, Dorval M, Rivoal J. 2018. *Arabidopsis thaliana* alcohol dehydrogenase is differently affected by several redox modifications. *PLoS ONE* **13**: e0204530.

Elhafez D, Murcha MW, Clifton R, Soole KL, Day DA, Whelan J. 2006. Characterization of mitochondrial alternative NAD(P)H dehydrogenases in Arabidopsis: intraorganelle location and expression. *Plant and Cell Physiology* **47**: 43–54.

Elstner EF, Osswald W. 1994. Mechanisms of oxygen activation during plant stress. *Proceedings of the Royal Society of Edinburgh. Section B: Biological Sciences* **102**: 131–154.

Escobar MA, Franklin KA, Svensson ÅS, Salter MG, Whitelam GC, Rasmusson AG. 2004. Light regulation of the Arabidopsis respiratory chain. Multiple discrete photoreceptor responses contribute to induction of type II NAD(P)H dehydrogenase genes. *Plant Physiology* **136**: 2710–2721.

Escobar MA, Geisler DA, Rasmusson AG. 2006. Reorganization of the alternative pathways of the Arabidopsis respiratory chain by nitrogen supply: opposing effects of ammonium and nitrate. *The Plant Journal* **45**: 775–788.

Fuchs P, Bohle F, Lichtenauer S, Ugalde JM, Feitosa Araujo E, Mansuroglu B, Ruberti C, Wagner S, Müller-Schüssele SJ, Meyer AJ *et al.* 2022. Reductive stress triggers ANAC017-mediated retrograde signaling to safeguard the endoplasmic reticulum by boosting mitochondrial respiratory capacity. *Plant Cell* **34**: 1375–1395.

Fukao T, Yeung E, Bailey-Serres J. 2011. The submergence tolerance regulator SUB1A mediates crosstalk between submergence and drought tolerance in rice. *Plant Cell* **23**: 412–427.

Garnczarska M, Bednarski W, Morkunas I. 2004. Re-aeration–induced oxidative stress and antioxidative defenses in hypoxically pretreated lupine roots. *Journal of Plant Physiology* **161**: 415–422.

Giraud E, Ho LHM, Clifton R, Carroll A, Estavillo G, Tan Y-F, Howell KA, Ivanova A, Pogson BJ, Millar AH. 2008. The absence of ALTERNATIVE OXIDASE1a in Arabidopsis results in acute sensitivity to combined light and drought stress. *Plant Physiology* **147**: 595–610.

Huang S, Van Aken O, Schwarzländer M, Belt K, Millar AH. 2016. The roles of mitochondrial reactive oxygen species in cellular signaling and stress response in plants. *Plant Physiology* **171**: 1551–1559.

Hung YP, Albeck JG, Tantama M, Yellen G. 2011. Imaging cytosolic NADH-NAD^+ redox state with a genetically encoded fluorescent biosensor. *Cell Metabolism* **14**: 545–554.

Jayawardhane J, Cochrane DW, Vyas P, Bykova NV, Vanlerberghe GC, Igamberdiev AU. 2020. Roles for plant mitochondrial alternative oxidase under normoxia, hypoxia, and reoxygenation conditions. *Frontiers in Plant Science* **11**: 566.

Jethva J, Schmidt RR, Sauter M, Selinski J. 2022. Try or die: dynamics of plant respiration and how to survive low oxygen conditions. *Plants* **11**: 205.

Karimi M, Inzé D, Depicker A. 2002. GATEWAY™ vectors for *Agrobacterium*-mediated plant transformation. *Trends in Plant Science* **7**: 193–195.

Kato Y, Collard BCY, Septiningsih EM, Ismail AM. 2014. Physiological analyses of traits associated with tolerance of long-term partial submergence in rice. *AoB Plants* **6**: plu058.

Khan MN, Komatsu S. 2016. Characterization of post-flooding recovery-responsive enzymes in soybean root and hypocotyl. *Journal of Plant Biology* **59**: 478–487.

Khan MN, Sakata K, Hiraga S, Komatsu S. 2014. Quantitative proteomics reveals that peroxidases play key roles in post-flooding recovery in soybean roots. *Journal of Proteome Research* **13**: 5812–5828.

Kim S-Y, Kim S-G, Kim Y-S, Seo PJ, Bae M, Yoon H-K, Park C-M. 2006. Exploring membrane-associated NAC transcription factors in Arabidopsis: implications for membrane biology in genome regulation. *Nucleic Acids Research* **35**: 203–213.

Kim Y-S, Sakuraba Y, Han S-H, Yoo S-C, Paek N-C. 2013. Mutation of the Arabidopsis NAC016 transcription factor delays leaf senescence. *Plant and Cell Physiology* **54**: 1660–1672.

Kozaki A, Takeba G. 1996. Photorespiration protects C_3 plants from photooxidation. *Nature* **384**: 557–560.

Lassowskat I, Hartl M, Hosp F, Boersema PJ, Mann M, Finkemeier I. 2017. Dimethyl-labeling-based quantification of the lysine acetylome and proteome of plants. *Methods in Molecular Biology* **1653**: 65–81.

Licausi F, Kosmacz M, Weits DA, Giuntoli B, Giorgi FM, Voesenek LACJ, Perata P, van Dongen JT. 2011. Oxygen sensing in plants is mediated by an N-end rule pathway for protein destabilization. *Nature* **479**: 419–422.

Lichtenthaler HK. 1987. Chlorophylls and carotenoids: pigments of photosynthetic biomembranes. *Methods in Enzymology* **148**: 350–382.

Liu Z, Hartman S, van Veen H, Zhang H, Leeggangers HACF, Martopawiro S, Bosman F, de Deugd F, Su P, Hummel M *et al.* 2022. Ethylene augments root hypoxia tolerance via growth cessation and reactive oxygen species amelioration. *Plant Physiology* **190**: 1365–1383.

Luo F-L, Matsubara S, Chen Y, Wei G-W, Dong B-C, Zhang M-X, Yu F-H. 2018. Consecutive submergence and de-submergence both impede growth of a riparian plant during water level fluctuations with different frequencies. *Environmental and Experimental Botany* **155**: 641–649.

Luo F-L, Nagel KA, Scharr H, Zeng B, Schurr U, Matsubara S. 2010. Recovery dynamics of growth, photosynthesis and carbohydrate accumulation after de-submergence: a comparison between two wetland plants showing escape and quiescence strategies. *Annals of Botany* **107**: 49–63.

Luo F-L, Nagel KA, Zeng B, Schurr U, Matsubara S. 2009. Photosynthetic acclimation is important for post-submergence recovery of photosynthesis and growth in two riparian species. *Annals of Botany* **104**: 1435–1444.

Maxwell DP, Wang Y, McIntosh L. 1999. The alternative oxidase lowers mitochondrial reactive oxygen production in plant cells. *Proceedings of the National Academy of Sciences, USA* **96**: 8271–8276.

Meng X, Li L, De Clercq I, Narsai R, Xu Y, Hartmann A, Claros DL, Custovic E, Lewsey MG, Whelan J *et al.* 2019. ANAC017 coordinates organellar functions and stress responses by reprogramming retrograde signaling. *Plant Physiology* **180**: 634–653.

Meng X, Li L, Narsai R, De Clercq I, Whelan J, Berkowitz O. 2020. Mitochondrial signaling is critical for acclimation and adaptation to flooding in *Arabidopsis thaliana*. *The Plant Journal* **103**: 227–247.

Michalecka AM, Svensson ÅS, Johansson FI, Agius SC, Johanson U, Brennicke A, Binder S, Rasmusson AG. 2003. Arabidopsis genes encoding mitochondrial type II NAD(P)H dehydrogenases have different evolutionary origin and show distinct responses to light. *Plant Physiology* **133**: 642–652.

Millar AH, Trend AE, Heazlewood JL. 2004. Changes in the mitochondrial proteome during the anoxia to air transition in rice focus around cytochrome-containing respiratory complexes. *Journal of Biological Chemistry* **279**: 39471–39478.

Mittler R, Zandalinas SI, Fichman Y, Van Breusegem F. 2022. Reactive oxygen species signaling in plant stress responses. *Nature Reviews Molecular Cell Biology* **23**: 663–679.

Møller IM. 2001. Plant mitochondria and oxidative stress: electron transport, NADPH turnover, and metabolism of reactive oxygen species. *Annual Review of Plant Physiology and Plant Molecular Biology* **52**: 561–591.

Møller IM, Igamberdiev AU, Bykova NV, Finkemeier I, Rasmusson AG, Schwarzländer M. 2020. Matrix redox physiology governs the regulation of plant mitochondrial metabolism through posttranslational protein modifications. *Plant Cell* **32**: 573–594.

Møller IM, Jensen PE, Hansson A. 2007. Oxidative modifications to cellular components in plants. *Annual Review of Plant Biology* **58**: 459–481.

Møller IM, Rasmusson AG, Van Aken O. 2021. Plant mitochondria – past, present and future. *The Plant Journal* **108**: 912–959.

Møller IM, Sweetlove LJ. 2010. ROS signaling–specificity is required. *Trends in Plant Science* **15**: 370–374.

Monk LS, Fagerstedt KV, Crawford RMM. 1987. Superoxide dismutase as an anaerobic polypeptide: a key factor in recovery from oxygen deprivation in *Iris pseudacorus*? *Plant Physiology* **85**: 1016–1020.

Moore CS, Cook-Johnson RJ, Rudhe C, Whelan J, Day DA, Wiskich JT, Soole KL. 2003. Identification of *AtNDI1*, an internal non-phosphorylating NAD(P)H dehydrogenase in Arabidopsis mitochondria. *Plant Physiology* **133**: 1968–1978.

Murphy MP. 2009. How mitochondria produce reactive oxygen species. *Biochemical Journal* **417**: 1–13.

Narsai R, Howell KA, Carroll A, Ivanova A, Millar AH, Whelan J. 2009. Defining core metabolic and transcriptomic responses to oxygen availability in rice embryos and young seedlings. *Plant Physiology* **151**: 306–322.

Ng S, De Clercq I, Van Aken O, Law SR, Ivanova A, Willems P, Giraud E, Van Breusegem F, Whelan J. 2014. Anterograde and retrograde regulation of nuclear genes encoding mitochondrial proteins during growth, development, and stress. *Molecular Plant* **7**: 1075–1093.

Ng S, Ivanova A, Duncan O, Law SR, Van Aken O, De Clercq I, Wang Y, Carrie C, Xu L, Kmiec B *et al.* 2013. A membrane-bound NAC transcription factor, ANAC017, mediates mitochondrial retrograde signaling in *Arabidopsis thaliana*. *Plant Cell* **25**: 3450–3471.

Nietzel T, Elsässer M, Ruberti C, Steinbeck J, Ugalde JM, Fuchs P, Wagner S, Ostermann L, Moseler A, Lemke P *et al.* 2019. The fluorescent protein sensor roGFP2-Orp1 monitors *in vivo* H_2O_2 and thiol redox integration and elucidates intracellular H_2O_2 dynamics during elicitor-induced oxidative burst in Arabidopsis. *New Phytologist* **221**: 1649–1664.

O'Donnell A, Harvey LM, McNeil B. 2011. The roles of the alternative NADH dehydrogenases during oxidative stress in cultures of the filamentous fungus *Aspergillus niger*. *Fungal Biology* **115**: 359–369.

Olsen AN, Ernst HA, Leggio LL, Skriver K. 2005. NAC transcription factors: structurally distinct, functionally diverse. *Trends in Plant Science* **10**: 79–87.

Pavelic D, Arpagaus S, Rawyler A, Brändle R. 2000. Impact of post-anoxia stress on membrane lipids of anoxia-pretreated potato cells. A re-appraisal. *Plant Physiology* **124**: 1285–1292.

Pérez-Pérez ME, Lemaire SD, Crespo JL. 2012. Reactive oxygen species and autophagy in plants and algae. *Plant Physiology* **160**: 156–164.

Popov VN, Syromyatnikov MY, Fernie AR, Chakraborty S, Gupta KJ, Igamberdiev AU. 2021. The uncoupling of respiration in plant mitochondria: keeping reactive oxygen and nitrogen species under control. *Journal of Experimental Botany* **72**: 793–807.

Pospíšil P. 2009. Production of reactive oxygen species by photosystem II. *Biochimica et Biophysica Acta (BBA) – Bioenergetics* **1787**: 1151–1160.

Prasad TK, Anderson MD, Martin BA, Stewart CR. 1994. Evidence for chilling-induced oxidative stress in maize seedlings and a regulatory role for hydrogen peroxide. *Plant Cell* **6**: 65–74.

Pucciariello C, Perata P. 2021. The oxidative paradox in low oxygen stress in plants. *Antioxidants* **10**: 332.

Rasmusson AG, Escobar MA. 2007. Light and diurnal regulation of plant respiratory gene expression. *Physiologia Plantarum* **129**: 57–67.

Rasmusson AG, Geisler DA, Møller IM. 2008. The multiplicity of dehydrogenases in the electron transport chain of plant mitochondria. *Mitochondrion* **8**: 47–60.

Rasmusson AG, Møller IM. 1991. NAD(P)H dehydrogenases on the inner surface of the inner mitochondrial membrane studied using inside-out submitochondrial particles. *Physiologia Plantarum* **83**: 357–365.

Santosa IE, Ram PC, Boamfa EI, Laarhoven LJJ, Reuss J, Jackson MB, Harren FJM. 2007. Patterns of peroxidative ethane emission from submerged rice seedlings indicate that damage from reactive oxygen species takes place during submergence and is not necessarily a post-anoxic phenomenon. *Planta* **226**: 193–202.

Sasidharan R, Bailey-Serres J, Ashikari M, Atwell BJ, Colmer TD, Fagerstedt K, Fukao T, Geigenberger P, Hebelstrup KH, Hill RD *et al.* 2017. Community recommendations on terminology and procedures used in flooding and low oxygen stress research. *New Phytologist* **214**: 1403–1407.

Schertl P, Braun H-P. 2014. Respiratory electron transfer pathways in plant mitochondria. *Frontiers in Plant Science* **5**: 163.

Selinski J, Scheibe R, Day DA, Whelan J. 2018. Alternative oxidase is positive for plant performance. *Trends in Plant Science* **23**: 588–597.

Seo PJ, Kim S-G, Park C-M. 2008. Membrane-bound transcription factors in plants. *Trends in Plant Science* **13**: 550–556.

Shapiguzov A, Nikkanen L, Fitzpatrick D, Vainonen JP, Tiwari A, Gossens R, Alseekh S, Aarabi F, Blokhina O, Panzarová K *et al.* 2019a. Increased expression of mitochondrial dysfunction stimulon genes affects chloroplast redox status and photosynthetic electron transfer in Arabidopsis. *bioRxiv*. doi: 10.1101/696740.

Shapiguzov A, Vainonen JP, Hunter K, Tossavainen H, Tiwari A, Järvi S, Hellman M, Aarabi F, Alseekh S, Wybouw B. 2019b. Arabidopsis RCD1 coordinates chloroplast and mitochondrial functions through interaction with ANAC transcription factors. *eLife* **8**: e43284.

Smirnoff H. 1995. Antioxidant systems and plant response to the environment. In: Smirnoff V, ed. *Environment and plant metabolism: flexibility and acclimation*. Oxford, UK: BIOS Scientific, 217–243.

Sone C, Sakagami J-I. 2017. Physiological mechanism of chlorophyll breakdown for leaves under complete submergence in rice. *Crop Science* **57**: 2729–2738.

Steinbeck J, Fuchs P, Negroni YL, Elsässer M, Lichtenauer S, Stockdreher Y, Feitosa-Araujo E, Kroll JB, Niemeier J-O, Humberg C *et al.* 2020. *In vivo* NADH/NAD^+ biosensing reveals the dynamics of cytosolic redox metabolism in plants. *Plant Cell* **32**: 3324–3345.

Svensson ÅS, Rasmusson AG. 2001. Light-dependent gene expression for proteins in the respiratory chain of potato leaves. *The Plant Journal* **28**: 73–82.

Sweetman C, Waterman CD, Rainbird BM, Smith PMC, Jenkins CD, Day DA, Soole KL. 2019. AtNDB2 is the main external NADH dehydrogenase in mitochondria and is important for tolerance to environmental stress. *Plant Physiology* **181**: 774–788.

Tran L-SP, Nakashima K, Sakuma Y, Simpson SD, Fujita Y, Maruyama K, Fujita M, Seki M, Shinozaki K, Yamaguchi-Shinozaki K. 2004. Isolation and functional analysis of Arabidopsis stress-inducible NAC transcription factors that bind to a drought-responsive *cis*-element in the *early responsive to dehydration stress 1* promoter. *Plant Cell* **16**: 2481–2498.

Tsai K-J, Chou S-J, Shih M-C. 2014. Ethylene plays an essential role in the recovery of Arabidopsis during post-anaerobiosis reoxygenation. *Plant, Cell & Environment* **37**: 2391–2405.

Tsai K-J, Lin C-Y, Ting C-Y, Shih M-C. 2016. Ethylene-regulated glutamate dehydrogenase fine-tunes metabolism during anoxia-reoxygenation. *Plant Physiology* **172**: 1548–1562.

Ugalde JM, Aller I, Kudrjasova L, Schmidt RR, Schlößer M, Homagk M, Fuchs P, Lichtenauer S, Schwarzländer M, Müller-Schüssele SJ *et al.* 2022. Endoplasmic reticulum oxidoreductin provides resilience against reductive stress and hypoxic conditions by mediating luminal redox dynamics. *Plant Cell* **34**: 4007–4027.

Ugalde JM, Fuchs P, Nietzel T, Cutolo EA, Homagk M, Vothknecht UC, Holuigue L, Schwarzländer M, Müller-Schüssele SJ, Meyer AJ. 2021. Chloroplast-derived photo-oxidative stress causes changes in H_2O_2 and E_{GSH} in other subcellular compartments. *Plant Physiology* **186**: 125–141.

Van Aken O, De Clercq I, Ivanova A, Law SR, Van Breusegem F, Millar AH, Whelan J. 2016a. Mitochondrial and chloroplast stress responses are modulated in distinct touch and chemical inhibition phases. *Plant Physiology* **171**: 2150–2165.

Van Aken O, Ford E, Lister R, Huang S, Millar AH. 2016b. Retrograde signaling caused by heritable mitochondrial dysfunction is partially mediated by ANAC017 and improves plant performance. *The Plant Journal* **88**: 542–558.

Vanlerberghe GC, Dahal K, Alber NA, Chadee A. 2020. Photosynthesis, respiration and growth: a carbon and energy balancing act for alternative oxidase. *Mitochondrion* **52**: 197–211.

Vanlerberghe GC, Martyn GD, Dahal K. 2016. Alternative oxidase: a respiratory electron transport chain pathway essential for maintaining photosynthetic performance during drought stress. *Physiologia Plantarum* **157**: 322–337.

Vanlerberghe GC, McIntosh L. 1997. Alternative oxidase: from gene to function. *Annual Review of Plant Biology* **48**: 703–734.

Vanlerberghe GC, McLntosh L. 1996. Signals regulating the expression of the nuclear gene encoding alternative oxidase of plant mitochondria. *Plant Physiology* **111**: 589–595.

Vercesi AE, Borecký J, Maia IG, Arruda P, Cuccovia IM, Chaimovich H. 2006. Plant uncoupling mitochondrial proteins. *Annual Review of Plant Biology* **57**: 383–404.

Vishwakarma A, Tetali SD, Selinski J, Scheibe R, Padmasree K. 2015. Importance of the alternative oxidase (AOX) pathway in regulating cellular redox and ROS homeostasis to optimize photosynthesis during restriction of the cytochrome oxidase pathway in *Arabidopsis thaliana*. *Annals of Botany* **116**: 555–569.

Wagner S, Steinbeck J, Fuchs P, Lichtenauer S, Elsässer M, Schippers JHM, Nietzel T, Ruberti C, Van Aken O, Meyer AJ. 2019. Multiparametric real-time sensing of cytosolic physiology links hypoxia responses to mitochondrial electron transport. *New Phytologist* **224**: 1668–1684.

Wagner S, Van Aken O, Elsässer M, Schwarzländer M. 2018. Mitochondrial energy signaling and its role in the low-oxygen stress response of plants. *Plant Physiology* **176**: 1156–1170.

Wallström SV, Florez-Sarasa I, Araújo WL, Escobar MA, Geisler DA, Aidemark M, Lager I, Fernie AR, Ribas-Carbó M, Rasmusson AG. 2014. Suppression of NDA-type alternative mitochondrial NAD(P)H dehydrogenases in *Arabidopsis thaliana* modifies growth and metabolism, but not high light stimulation of mitochondrial electron transport. *Plant and Cell Physiology* **55**: 881–896.

Wang Y, Berkowitz O, Selinski J, Xu Y, Hartmann A, Whelan J. 2018. Stress responsive mitochondrial proteins in *Arabidopsis thaliana*. *Free Radical Biology and Medicine* **122**: 28–39.

Yamada S, Ozaki H, Noguchi K. 2020. The mitochondrial respiratory chain maintains the photosynthetic electron flow in *Arabidopsis thaliana* leaves under high-light stress. *Plant & Cell Physiology* **61**: 283–295.

Yang C-Y. 2014. Hydrogen peroxide controls transcriptional responses of ERF73/HRE1 and ADH1 via modulation of ethylene signaling during hypoxic stress. *Planta* **239**: 877–885.

Yang L, Zhang J, He J, Qin Y, Hua D, Duan Y, Chen Z, Gong Z. 2014. ABA-mediated ROS in mitochondria regulate root meristem activity by controlling *PLETHORA* expression in *Arabidopsis*. *PLoS Genetics* **10**: e1004791.

Yeung E, Bailey-Serres J, Sasidharan R. 2019. After the deluge: plant revival post-flooding. *Trends in Plant Science* **24**: 443–454.

Yeung E, van Veen H, Vashisht D, Sobral Paiva AL, Hummel M, Rankenberg T, Steffens B, Steffen-Heins A, Sauter M, de Vries M *et al.* 2018. A stress recovery signaling network for enhanced flooding tolerance in *Arabidopsis thaliana*. *Proceedings of the National Academy of Sciences, USA* **115**: E6085–E6094.

Yuan L-B, Dai Y-S, Xie L-J, Yu L-J, Zhou Y, Lai Y-X, Yang Y-C, Xu L, Chen Q-F, Xiao S. 2017. Jasmonate regulates plant responses to postsubmergence reoxygenation through transcriptional activation of antioxidant synthesis. *Plant Physiology* **173**: 1864–1880.

Zarkovic J, Anderson SL, Rhoads DM. 2005. A reporter gene system used to study developmental expression of alternative oxidase and isolate mitochondrial retrograde regulation mutants in Arabidopsis. *Plant Molecular Biology* **57**: 871–888.

Supporting Information

Additional Supporting Information may be found online in the Supporting Information section at the end of the article.

Fig. S1 Expression of *Arabidopsis thaliana* type II NADH dehydrogenase and alternative oxidase genes under abiotic stresses based on Genevestigator data.

Fig. S2 Schematic representation of *NDA1*, *NDA2*, *ANAC016*, and *ANAC017* gene structures.

Fig. S3 Expression analysis of *NDA1* and *NDA2* using RT-qPCR.

Fig. S4 Representative pictures of wild-type, single and double *NDA* knockout, NDA overexpression, *anac016* and *anac017-1* seedlings.

Fig. S5 Analysis of *nda1-1 nda2-2* complementation lines genetically link *NDA* gene expression to plant survival of reoxygenation.

Fig. S6 Representative pictures of wild-type, *nda1-1 nda2-2*, and seedlings of the complementation lines generated in the *nda1-1 nda2-2* background after recovery from anoxia.

Fig. S7 Quantitative protein profiling of NDA1 and NDA2 from isolated mitochondria of wild-type, *nda1-1 nda2-2*, *NDA1ox3*, and *NDA2ox2* shoots.

Fig. S8 *NDA1* and *NDA2* are upregulated by reoxygenation.

Fig. S9 ANAC013, ANAC016, and ANAC017 do not activate the *NDA2* promoter.

Fig. S10 Reactive oxygen species production in cytosol and mitochondria under changing O_2 conditions.

Methods S1 Plant material, growth conditions, and plant treatments.

Methods S2 Mitochondria isolation and LC–MS/MS-based quantitative proteome analyses.

Methods S3 Reactive oxygen species analysis using DAB and NBT staining and EPR spectroscopy.

Methods S4 Measurement of ATP, NAD reduction level, and H_2O_2 concentration with fluorescent biosensors.

Methods S5 Histochemical GUS analysis.

Methods S6 Adenylate measurements by LC–MS.

Methods S7 Statistical evaluation.

Table S1 Primers used for genotyping, cloning, and RT-qPCR (qPCR) analyses.

Table S2 Primers used to generate probes for EMSA.

Please note: Wiley is not responsible for the content or functionality of any Supporting Information supplied by the authors. Any queries (other than missing material) should be directed to the *New Phytologist* Central Office.